Theory of helimagnons in itinerant quantum systems

D. Belitz,[1,2] T. R. Kirkpatrick,[1,3] and A. Rosch[4]
[1]*Kavli Institute for Theoretical Physics, University of California, Santa Barbara, California 93106, USA*
[2]*Department of Physics and Materials Science Institute, University of Oregon, Eugene, Oregon 97403, USA*
[3]*Institute for Physical Science and Technology, and Department of Physics, University of Maryland, College Park, Maryland 20742, USA*
[4]*Institut für Theoretische Physik, Universität zu Köln, Zülpicher Strasse 77, D-50937 Köln, Germany*
(Received 18 October 2005; revised manuscript received 13 December 2005; published 24 February 2006)

The nature and effects of the Goldstone mode in the ordered phase of helical or chiral itinerant magnets such as MnSi are investigated theoretically. It is shown that the Goldstone mode, or helimagnon, is a propagating mode with a highly anisotropic dispersion relation, in analogy to the Goldstone mode in chiral liquid crystals. Starting from a microscopic theory, a comprehensive effective theory is developed that allows for an explicit description of the helically ordered phase, including the helimagnons, for both classical and quantum helimagnets. The directly observable dynamical spin susceptibility, which reflects the properties of the helimagnon, is calculated.

DOI: 10.1103/PhysRevB.73.054431 PACS number(s): 75.30.Ds, 75.50.−y, 75.25.+z

I. INTRODUCTION

Ferromagnetism and antiferromagnetism are the most common and well-known examples of long-range magnetic order in solids. The metallic ferromagnets Fe and Ni in particular are among the most important and well-studied magnetic materials. In the ordered phase, where the rotational symmetry in spin space is spontaneously broken, one finds soft modes in accordance with Goldstone's theorem: namely, ferromagnetic magnons. The latter are propagating modes with a dispersion relation, or frequency-wave vector relation, $\mathbf{\Omega} \sim \boldsymbol{k}^2$ in the long-wavelength limit. In antiferromagnets, the corresponding antiferromagnetic magnons have a dispersion relation $\mathbf{\Omega} \sim |\boldsymbol{k}|$. In rotationally invariant models that ignore the spin-orbit coupling of the electronic spin to the underlying lattice structure these relations hold to arbitrarily small frequencies Ω and wave vectors $\boldsymbol{k}$. The lattice structure ultimately breaks the rotational symmetry and gives the Goldstone modes a mass. In ferromagnets, the low-energy dispersion relation is also modified by the induced magnetic field, which generates a domain structure. These are very small effects, however, and magnons that are soft for all practical purposes are clearly observed, directly via neutron scattering and indirectly via their contribution to, e.g., the specific heat.[1] These observations illustrate important concepts of symmetries in systems with many degrees of freedom with ramifications that go far beyond the realm of solid-state physics.[2,3]

In systems where the lattice lacks inversion symmetry additional effects occur that are independent of the spin rotational symmetry. This is due to terms in the action that are invariant under simultaneous rotations of real space and $\boldsymbol{M}$, with $\boldsymbol{M}$ the magnetic order parameter, but break spatial inversion symmetry. Microscopically, such terms arise from the spin-orbit interaction and their precise functional form depends on the lattice structure. One important class of such terms, which is realized in the metallic compound MnSi, is of the form $\boldsymbol{M} \cdot (\boldsymbol{\nabla} \times \boldsymbol{M})$.[4,5] They are known to lead to helical or spiral order in the ground state, where the magnetization is ferromagnetically ordered in the planes perpendicular to some direction $\boldsymbol{q}$, with a helical modulation of wavelength $2\pi/|\boldsymbol{q}|$ along the $\boldsymbol{q}$ axis.[6,7] In MnSi, which displays helical order below a temperature $T_c \approx 30$ K at ambient pressure, $2\pi/|\boldsymbol{q}| \approx 180$ Å.[8] Application of hydrostatic pressure p suppresses T_c, which goes to zero at a critical pressure $p_c \approx 14$ kbar.[9]

In addition to the helical order, which is well understood, MnSi shows many strange properties that have attracted much attention lately and so far lack explanations. Arguably the most prominent of these features is a pronounced non-Fermi-liquid behavior of the resistivity in the disordered phase at low temperatures for $p > p_c$.[10] In part of the region where non-Fermi-liquid behavior is observed, neutron scattering shows "partial" magnetic order where helices still exist on intermediate length scales but have lost their long-range directional order.[11] Such non-Fermi-liquid behavior is not observed in other low-temperature magnets. Since the helical order is the only obvious feature that sets MnSi apart from these other materials, it is natural to speculate that there is some connection between the helical order and the transport anomalies. In this context it is surprising that some basic properties and effects of the helically ordered state, and in particular of the helical Goldstone mode, which we will refer to as a *helimagnon* in analogy to the ferromagnons and antiferromagnons mentioned above, are not known. The purpose of the present paper is to address this issue. We will identify the helimagnon and determine its properties, in particular its dispersion relation and damping properties. We also calculate the spin susceptibility, which is directly observable and simply related to the helimagnon. The effects of this soft mode on various other observables will be explored in a separate paper.[12] A brief account of some of our results, as well as some of their consequences, has been given in Ref. 13.

One of our goals is to develop an effective theory for itinerant quantum helimagnets. We will do so by deriving a quantum Ginzburg-Landau theory whose coefficients are given in terms of microscopic electronic correlation functions. Such a theory has two advantages over a purely phenomenological treatment based on symmetry arguments alone. First, it allows for a semiquantitative analysis, since the coefficients of the Ginzburg-Landau theory can be expressed in terms of microscopic parameters. Second, it derives all of the ingredients necessary for calculating the thermodynamic and transport properties of an itinerant helimagnet in the ordered phase using many-body perturbation theory techniques.[12]

The organization of the remainder of this paper is as follows. In Sec. II we use an analogy with chiral liquid crystals to make an educated guess about the wave vector dependence of fluctuations in helimagnets and employ time-dependent Ginzburg-Landau theory to find the dynamics. In Sec. III we derive the static properties from a classical Ginzburg-Landau theory. In Sec. IV we start with a microscopic quantum mechanical description and derive an effective quantum theory for chiral magnets. We then show that all of the qualitative results obtained from the simple arguments in Sec. II follow from this theory, with the additional benefit that parameter values can be determined semiquantitatively. We conclude in Sec. V with a summary and a discussion of our results. Some technical details are relegated to three appendixes.

II. SIMPLE PHYSICAL ARGUMENTS AND RESULTS

Helimagnets are not the only macroscopic systems that display chirality; another example is cholesteric liquid crystals whose director order parameter is arranged in a helical pattern analogous to that followed by the magnetization in a helimagnet.[14] There are some important differences between magnets and liquid crystals. For instance, the two orientations of the director order parameter in the latter are equivalent, which necessitates a description in terms of a rank-2 tensor, rather than a vector as in magnets.[15] Also, the chirality in cholesteric liquid crystals is a consequence of the chiral properties of the constituting molecules, whereas in magnets it is a result of interactions between the electrons and atoms of the underlying lattice. However, these differences are not expected to be relevant for some basic properties of the Goldstone mode that must be present in the helical state of either system.[16] We will therefore start by using the known hydrodynamic properties of cholesteric liquid crystals to motivate a guess of the nature of the Goldstone mode in helimagnets. In Sec. III we will see that the results obtained in this way are indeed confirmed by an explicit calculation. The arguments employed in this section are phenomenological in nature and very general. We therefore expect them to apply equally to classical helimagnets and to quantum helimagnets at $T=0$, as is the case for analogous arguments for ferromagnetic and antiferromagnetic magnons.

A. Statics

Consider a classical magnet with an order parameter field $\boldsymbol{M}(\boldsymbol{x})$ and an action[6,7]

$$S[\boldsymbol{M}] = \int d\boldsymbol{x}\left[\frac{r}{2}\boldsymbol{M}^2(\boldsymbol{x}) + \frac{a}{2}[\nabla \boldsymbol{M}(\boldsymbol{x})]^2 + \frac{c}{2}\boldsymbol{M}(\boldsymbol{x})\cdot[\boldsymbol{\nabla}\times\boldsymbol{M}(\boldsymbol{x})] + \frac{u}{4}[\boldsymbol{M}^2(\boldsymbol{x})]^2\right]. \tag{2.1}$$

This is a classical ϕ^4 theory with a chiral term with coupling constant c. Physically, c is proportional to the spin-orbit coupling strength g_{SO}. The expectation value of $\boldsymbol{M}$ is proportional to the magnetization, and it is easy to see that a helical field configuration constitutes a saddle-point solution of the action given by Eq. (2.1),

$$\boldsymbol{M}_{\mathrm{sp}}(\boldsymbol{x}) = m_0(\boldsymbol{e}_1 \cos \boldsymbol{q}\cdot\boldsymbol{x} + \boldsymbol{e}_2 \sin \boldsymbol{q}\cdot\boldsymbol{x}) \tag{2.2a}$$

$$= m_0(\cos qz, \sin qz, 0). \tag{2.2b}$$

In Eq. (2.2a), $\boldsymbol{e}_1$ and $\boldsymbol{e}_2$ are two unit vectors that are perpendicular to each other and to the pitch vector $\boldsymbol{q}$. The chirality of the dreibein $\{\boldsymbol{q},\boldsymbol{e}_1,\boldsymbol{e}_2\}$ reflects the chirality of the underlying lattice structure and is encoded in the coefficient c in Eq. (2.1), with the sign of c determining the handedness of the chiral structure. In Eq. (2.2b) we have chosen a coordinate system such that $\{\boldsymbol{e}_1,\boldsymbol{e}_2,\boldsymbol{q}/q\}=\{\hat{x},\hat{y},\hat{z}\}$, a choice we will use for all explicit calculations. We will further choose, without loss of generality, $c>0$. The free energy is minimized by $q=c/2a$, and the pitch wave number is thus proportional to g_{SO}.

Now consider fluctuations about this saddle point. An obvious guess for the soft mode associated with the ordered helical state are phase fluctuations of the form

$$\boldsymbol{M}(\boldsymbol{x}) = m_0(\cos[qz+\phi(\boldsymbol{x})], \sin[qz+\phi(\boldsymbol{x})], 0) = \boldsymbol{M}_{\mathrm{sp}}(\boldsymbol{x}) + m_0\phi(\boldsymbol{x})(-\sin qz, \cos qz, 0) + O(\phi^2). \tag{2.3}$$

These phase fluctuations are indeed soft; by substituting Eq. (2.3) in Eq. (2.1), one finds an effective action $S_{\mathrm{eff}}[\phi] = \mathrm{const}\times\int d\boldsymbol{x}[\boldsymbol{\nabla}\phi(\boldsymbol{x})]^2$. However, this cannot be the correct answer, which can be seen as follows.[17] Consider a simple rotation of the planes containing the spins such that their normal changes from $(0,0,q)$ to (α_1,α_2,q), which corresponds to a phase fluctuation $\phi(\boldsymbol{x})=\alpha_1 x+\alpha_2 y$. This cannot cost any energy, yet $(\boldsymbol{\nabla}\phi)^2=\alpha_1^2+\alpha_2^2\neq 0$ for this particular phase fluctuation. The problem is the dependence of the effective action on $\boldsymbol{\nabla}_\perp\phi$, where $\boldsymbol{\nabla}=(\boldsymbol{\nabla}_\perp,\partial_z)$. The soft mode must therefore be some generalized phase $u(\boldsymbol{x})$ with a schematic structure

$$u(\boldsymbol{x}) \sim \phi(\boldsymbol{x}) + \nabla_\perp\varphi(\boldsymbol{x}), \tag{2.4}$$

where $\varphi(\boldsymbol{x})$ represents the z component of the order parameter vector $\boldsymbol{M}(\boldsymbol{x})$. The lowest-order dependence on perpendicular gradients allowed by rotational invariance is $\boldsymbol{\nabla}_\perp^2 u$, and the extra term in u proportional to $\boldsymbol{\nabla}_\perp$ will ensure that this requirement is fulfilled. The correct effective action thus is expected to have the form

$$S_{\text{eff}}[u] = \frac{1}{2}\int d\boldsymbol{x}\{c_z[\partial_z u(\boldsymbol{x})]^2 + c_\perp[\boldsymbol{\nabla}_\perp^2 u(\boldsymbol{x})]^2/q^2\}, \quad (2.5)$$

where c_z and $c_\perp$ are elastic constants. The Goldstone mode corresponding to helical order must therefore have an anisotropic dispersion relation: it will be softer in the direction perpendicular to the pitch vector than in the longitudinal direction.[18] Separating wave vectors $\boldsymbol{k}=(\boldsymbol{k}_\perp, k_z)$ into transverse and longitudinal components, the longitudinal wave number will scale as the transverse wave number squared, $k_z \sim \boldsymbol{k}_\perp^2/q$. The factor $1/q^2$ in the transverse term in Eq. (2.5), which serves to ensure that the constants c_z and $c_\perp$ have the same dimension, is the natural length scale to enter at this point, since a nonzero pitch wave number is what is causing the anisotropy in the first place. A detailed calculation for cholesteric liquid crystals[19] shows that this is indeed the correct answer, and we will see in Sec. III that the same is true for helimagnets.

B. Dynamics

In order to determine the dynamics of the soft mode in a simple phenomenological fashion we utilize the framework of time-dependent Ginzburg-Landau theory.[20] Within this formalism, the kinetic equation for the time-dependent generalization of the magnetization field $\boldsymbol{M}$ reads

$$\partial_t \boldsymbol{M}(\boldsymbol{x},t) = -\gamma \boldsymbol{M}(\boldsymbol{x},t) \times \left.\frac{\delta S}{\delta \boldsymbol{M}(\boldsymbol{x})}\right|_{\boldsymbol{M}(\boldsymbol{x},t)} - \int d\boldsymbol{y} D(\boldsymbol{x}-\boldsymbol{y}) \left.\frac{\delta S}{\delta \boldsymbol{M}(\boldsymbol{y})}\right|_{\boldsymbol{M}(\boldsymbol{y},t)} + \boldsymbol{\zeta}(\boldsymbol{x},t), \quad (2.6)$$

with γ a constant. The first term describes the precession of a magnetic moment in the field provided by all other magnetic moments, D is a differential operator describing dissipation that we will specify in Sec. II C, and $\boldsymbol{\zeta}$ is a random Langevin force with zero mean, $\langle \boldsymbol{\zeta}(\boldsymbol{x},t)\rangle = 0$, and a second moment consistent with the fluctuation-dissipation theorem.

Now assume an equilibrium state given by Eq. (2.2b). In considering deviations from the equilibrium state we must take into account both the generalized phase modes at wave vector $\boldsymbol{q}$, which are soft since they are Goldstone modes, and the modes at zero wave vector, which are soft due to spin conservation. The latter we denote by $\boldsymbol{m}(\boldsymbol{x},t)$, and for the former we use Eq. (2.3),[21]

$$\boldsymbol{M}(\boldsymbol{x},t) = \boldsymbol{M}_{\text{sp}}(\boldsymbol{x}) + \boldsymbol{m}(\boldsymbol{x},t) + m_0 u(\boldsymbol{x},t)(-\sin qz, \cos qz, 0). \quad (2.7)$$

The action for u is the effective action given by Eq. (2.5), and the action for $\boldsymbol{m}$ is a renormalized Ginzburg-Landau action of which we will need only the Gaussian mass term. We thus write

$$S[\boldsymbol{m},u] = \frac{r_0}{2}\int d\boldsymbol{x}\boldsymbol{m}^2(\boldsymbol{x}) + S_{\text{eff}}[u]. \quad (2.8)$$

The mass r_0 of the zero-wave-number mode that appears here and in the remainder of this section is different from the coefficient r in Eq. (2.1), and we assume $r_0 > 0$.[22]

We now use the kinetic equation (2.6) to calculate the average deviations $\langle \boldsymbol{m}(\boldsymbol{x},t)\rangle$ and $\langle u(\boldsymbol{x},t)\rangle$ from the equilibrium state. For simplicity we suppress both the averaging brackets and the explicit time dependence in our notation, and for the time being we neglect the dissipative term. With summation over repeated indices implied, Eq. (2.6) yields

$$\partial_t m_3(\boldsymbol{x}) = -\gamma \epsilon_{3ij} M_{\text{sp}}^i(\boldsymbol{x}) \int d\boldsymbol{y} \frac{\delta S}{\delta u(\boldsymbol{y})}\frac{\delta u(\boldsymbol{y})}{\delta M_j(\boldsymbol{x})} = -\gamma m_0 \int d\boldsymbol{y} \frac{\delta S}{\delta u(\boldsymbol{y})}\left[\cos qz \frac{\partial u(\boldsymbol{y})}{\partial M_y(\boldsymbol{x})} - \sin qz \frac{\partial u(\boldsymbol{y})}{\partial M_x(\boldsymbol{x})}\right], \quad (2.9a)$$

and by using Eq. (2.7) in the identity

$$\delta(\boldsymbol{x}-\boldsymbol{y}) = \int dz \frac{\delta u(\boldsymbol{x})}{\delta M_i(z)}\frac{\delta M_i(z)}{\delta u(\boldsymbol{y})},$$

we find

$$m_0\left(-\sin qz \frac{\delta u(\boldsymbol{x})}{\delta M_x(\boldsymbol{y})} + \cos qz \frac{\delta u(\boldsymbol{x})}{\delta M_y(\boldsymbol{y})}\right) = \delta(\boldsymbol{x}-\boldsymbol{y}). \quad (2.9b)$$

Using Eq. (2.9b) in Eq. (2.9a) eliminates the integration, and using Eqs. (2.8) and (2.5) we find a relation between m_3 and u,

$$\partial_t m_3(\boldsymbol{x}) = -\gamma \frac{\delta S_{\text{eff}}}{\delta u(\boldsymbol{x})} = -\gamma(-c_z\partial_z^2 + c_\perp \boldsymbol{\nabla}_\perp^4/q^2)u(\boldsymbol{x}). \quad (2.10)$$

A second relation is obtained from the identity

$$\partial_t M_1(\boldsymbol{x}) = \int d\boldsymbol{y} \frac{\delta M_1(\boldsymbol{x})}{\delta u(\boldsymbol{y})}\partial_t u(\boldsymbol{y}).$$

By applying Eq. (2.6) to the left-hand side and using Eqs. (2.8) and (2.7), we obtain

$$\int d\boldsymbol{y} \frac{\delta M_1(\boldsymbol{x})}{\delta u(\boldsymbol{y})}\partial_t u(\boldsymbol{y}) = \gamma r_0 \int d\boldsymbol{y} \frac{\delta M_1(\boldsymbol{x})}{\delta u(\boldsymbol{y})} m_3(\boldsymbol{y})$$

or

$$\partial_t u(\boldsymbol{x}) = \gamma r_0 m_3(\boldsymbol{x}). \quad (2.11)$$

Combining Eqs. (2.10) and (2.11) we find a wave equation

$$\partial_t^2 u(\boldsymbol{x}) = -\gamma^2 r_0(-c_z\partial_z^2 + c_\perp \boldsymbol{\nabla}_\perp^4/q^2)u(\boldsymbol{x}). \quad (2.12)$$

This is the equation of motion for a harmonic oscillator with a resonance frequency

$$\omega_0(\boldsymbol{k}) = \gamma r_0^{1/2}\sqrt{c_z k_z^2 + c_\perp \boldsymbol{k}_\perp^4/q^2} \quad (2.13)$$

and a susceptibility

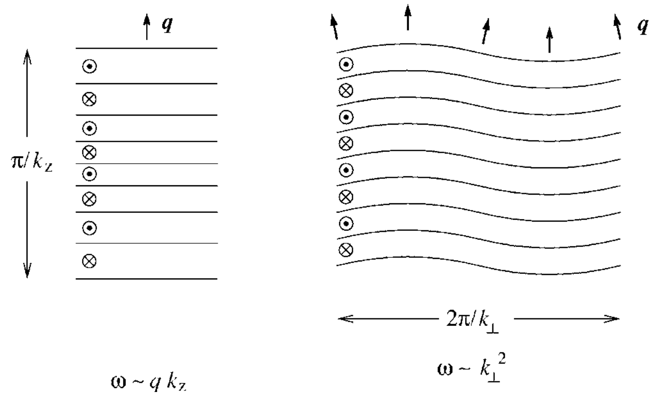

FIG. 1. Sketch of a longitudinal ($\boldsymbol{k} \parallel \boldsymbol{q}$, left panel) and transverse ($\boldsymbol{k} \perp \boldsymbol{q}$, right panel) helimagnon. The solid lines delineate planes of spins pointing out of (dotted circle) or into (crossed circle) the paper plane.

$$\chi_0 = \frac{1}{\omega_0^2(\boldsymbol{k}) - \omega^2}. \tag{2.14}$$

We thus have a propagating mode, the helimagnon, with an anisotropic dispersion relation: for wave vectors parallel to the pitch vector $\boldsymbol{q}$ the dispersion is linear, as in an antiferromagnet, while for wave vectors perpendicular to $\boldsymbol{q}$ it is quadratic. Fluctuations transverse with respect to the pitch vector are thus softer than longitudinal ones. The nature of the excitation corresponding to the longitudinal and transverse helimagnon, respectively, is shown in Fig. 1.

For later reference we note that for determining the static properties of the helimagnon it sufficed to discuss the phase modes at wave vector $\boldsymbol{q}$, while the dynamics are generated by a coupling between the phase modes and the modes at zero wave vector. This observation gives an important clue for the correct structure of the microscopic theory we will develop in Sec. IV.

C. Damping

In order to investigate the damping of the mode we need to take into account the dissipative term in the master equation (2.6) which we have neglected so far. Usually, in the case of a conserved order parameter, the damping operator D in Eq. (2.6) is proportional to a gradient squared.[20] In the present case, however, one expects an anisotropic differential operator, with different prefactors for the longitudinal and transverse parts, respectively. We will see in Sec. IV that in the particular model we will consider the transverse part of the gradient squared has a zero prefactor. We thus write

$$D(\boldsymbol{x}-\boldsymbol{y}) = \Gamma\,\delta(\boldsymbol{x}-\boldsymbol{y})\,\partial_z^2, \tag{2.15}$$

where Γ is a damping coefficient. Going through the derivation in the previous subsection again, we see that Eq. (2.11) remains unchanged except for gradient corrections to the right-hand side. Equation (2.10), on the other hand, acquires an additional term that is of the same order as the existing ones,

$$\partial_t m_3(\boldsymbol{x}) = -\gamma(-c_z\partial_z^2 + c_\perp \boldsymbol{\nabla}_\perp^4/q^2)u(\boldsymbol{x}) - r_0\Gamma\,\partial_z^2 m_3(\boldsymbol{x}). \tag{2.16}$$

Together with Eq. (2.11) this leads to an equation of motion for u given by

$$\partial_t^2 u(\boldsymbol{x}) = -\gamma^2 r_0(-c_z\partial_z^2 + c_\perp \boldsymbol{\nabla}_\perp^4/q^2)u(\boldsymbol{x}) - r_0\Gamma\,\partial_z^2\partial_t u(\boldsymbol{x}). \tag{2.17}$$

This corresponds to a damped harmonic oscillator with a susceptibility

$$\chi = \frac{1}{\omega_0^2(\boldsymbol{k}) - \omega^2 - i\omega\gamma(\boldsymbol{k})}, \tag{2.18a}$$

where the damping coefficient is given by

$$\gamma(\boldsymbol{k}) = r_0\Gamma k_z^2. \tag{2.18b}$$

Now recall that we are interested in systems where the magnetization is caused by itinerant electrons. In a system without any elastic scattering due to impurities and at zero temperature, the coefficient Γ, which physically is related to a generalized viscosity of the electron fluid, is itself wave number dependent and diverges for $\boldsymbol{k} \to 0$ as $\Gamma \propto 1/|\boldsymbol{k}|$. This leads to a damping coefficient

$$\gamma(\boldsymbol{k} \to 0) \propto k_z^2/|\boldsymbol{k}|. \tag{2.19a}$$

We see that $\gamma(\boldsymbol{k})$ scales as k_z (for $k_z^2 \gg \boldsymbol{k}_\perp^4/q^2$) or as $k_z^{3/2}$ (for $k_z^2 \ll \boldsymbol{k}_\perp^4/q^2$), while the resonance frequency ω_0 scales as k_z. If the prefactor of the damping coefficient is not too large, we thus have $\gamma(\boldsymbol{k}) < \omega_0(\boldsymbol{k})$ for all $\boldsymbol{k}$ and the mode is propagating. Any amount of quenched disorder will lead to Γ being finite at zero wave vector and hence to

$$\gamma(\boldsymbol{k} \to 0) \propto k_z^2. \tag{2.19b}$$

In this case, the mode is propagating at all wave vectors irrespective of the prefactor.

D. Physical spin susceptibility

The physical spin susceptibility χ_s, which is directly measurable, is given in terms of the order-parameter correlation function. The transverse (with respect to $\boldsymbol{q}$) components of χ_s are given by the correlations of the phase ϕ in Eq. (2.3) and are thus directly proportional to the Goldstone mode. In a schematic notation, which ignores the fact that ϕ at zero wave vector corresponds to a magnetization fluctuation at wave vector $\pm\boldsymbol{q}$, we thus expect

$$\chi_s^\perp(\boldsymbol{k},\omega) \propto \frac{1}{\omega_0^2(\boldsymbol{k}) - \omega^2 - i\omega\gamma(\boldsymbol{k})}. \tag{2.20a}$$

The longitudinal component will, by Eq. (2.4), carry an additional factor of $\boldsymbol{k}_\perp^2$ and is thus expected to have the structure

$$\chi_s^L(\boldsymbol{k},\omega) \propto \frac{\boldsymbol{k}_\perp^2}{\omega_0^2(\boldsymbol{k}) - \omega^2 - i\omega\gamma(\boldsymbol{k})}. \tag{2.20b}$$

Since $\omega \sim k_z \sim \boldsymbol{k}_\perp^2$ in a scaling sense, we see that the transverse susceptibility $\chi_s^\perp \sim 1/\omega^2$ is softer than the longitudinal one $\chi_s^L \sim 1/\omega$.

E. Effects of broken rotational and translational invariance

For the arguments given so far, the rotational symmetry of the action $S[\boldsymbol{M}]$, Eq. (2.1)—i.e., the invariance under simultaneous rotations in real space and spin space—played a crucial role. Since the underlying lattice structure of a real magnet breaks this symmetry, it is worthwhile to consider the consequences of this effect.

In a system with a cubic lattice like MnSi, the simplest term that breaks the rotational invariance is of the form[6,7]

$$S_{\text{cubic}}[\boldsymbol{M}] = \frac{a_1}{2}\int d\boldsymbol{x}\{[\partial_x M_x(\boldsymbol{x})]^2 + [\partial_y M_y(\boldsymbol{x})]^2 + [\partial_z M_z(\boldsymbol{x})]^2\}. \tag{2.21}$$

Other anisotropic terms with a cubic symmetry (see Appendix A for a complete list) have qualitatively the same effect. In Eq. (2.21), $a_1 \propto g_{\text{SO}}^2$, with g_{SO} the spin-orbit coupling strength (see Sec. II A). On dimensional grounds, we thus have $a_1 = bq^2 a$, with b a number and a the coefficient of the gradient squared term in Eq. (2.1). $b \neq 0$ leads to a pinning of the helix pitch vector in (1,1,1) or equivalent directions (for $b<0$) or in (1,0,0) or equivalent directions (for $b>0$).[6,7] In addition, it invalidates the argument in Sec. II A that there cannot be a $(\boldsymbol{\nabla}_\perp \phi)^2$ term in the effective action. However, the action is still translationally invariant, so a constant phase shift cannot cost any energy. To Eq. (2.1) we thus need to add a term

$$S_{\text{eff}}^{\text{cubic}}[u] = \frac{bq^2 a}{2}\int d\boldsymbol{x}[\boldsymbol{\nabla}_\perp u(\boldsymbol{x})]^2. \tag{2.22}$$

This changes the soft-mode frequency, Eq. (2.13), to

$$\omega_0(\boldsymbol{k}) = \gamma r_0^{1/2}\sqrt{c_z k_z^2 + baq^2\boldsymbol{k}_\perp^2 + c_\perp \boldsymbol{k}_\perp^4/q^2}. \tag{2.23}$$

We note that, due to the weakness of the spin-orbit coupling, $aq^2 \ll 1$, and therefore the breaking of the rotational symmetry is a very small effect. In MnSi, where the pitch wave length is on the order of 200 Å, while $a^{1/2}$ is on the order of a few Å at most, the presence of the $\boldsymbol{k}_\perp^2$ term is not observable with the current resolution of neutron scattering experiments, and we will ignore this term in the remainder of this paper.

The above considerations make it clear that the Goldstone mode is due to the spontaneous breaking of translational invariance, rather than rotational invariance in spin space. Consistent with this, there is only one Goldstone mode, as the helical state is still invariant under a two-parameter subgroup of the original three-parameter translational group.[23] In this sense, the helimagnon is more akin to phonons than to ferromagnetic magnons. Let us briefly discuss the effect of the ionic lattice on this symmetry, as the helix can be pinned by the periodic lattice potential and therefore one expects a gap in the magnetic excitation spectrum. To estimate the size of the gap, we investigate the low-energy theory taking into account only slowly varying modes with $|\boldsymbol{k}-\boldsymbol{q}| \lesssim q$. In a periodic lattice, momentum is conserved up to reciprocal lattice vectors $\boldsymbol{G_j}$. The leading term which breaks translational invariance, $\boldsymbol{M_k} \to \boldsymbol{M_k} e^{i\boldsymbol{k}\cdot\boldsymbol{r}_0}$, therefore is of the form

$$S_n = \sum_{\boldsymbol{k}_1,\ldots,\boldsymbol{k_n}\boldsymbol{j}} V_{\{\boldsymbol{k_l}\},\boldsymbol{G_j}} M_{\boldsymbol{k}_1} M_{\boldsymbol{k}_2}\cdots M_{\boldsymbol{k_n}} \delta\Big(\sum_i \boldsymbol{k_i} - \boldsymbol{G_j}\Big), \tag{2.24}$$

where V parametrizes the momentum-dependent coupling strength (and we have omitted vector indices). Within the low-energy theory, all momenta are of order of q. Therefore, umklapp scattering can only take place for $n \gtrsim G/q$. In the case of MnSi, where $G/q \approx 40$, one therefore needs a process proportional to M^{40} to create a finite gap. It is difficult to estimate the precise size of the gap which depends crucially, for example, on the commensuration of the helix with the underlying lattice. However, the resulting gap will in any case be unobservably small as it is exponentially suppressed by the large parameter $G/q \propto 1/g_{\text{SO}}$.

III. NATURE OF THE GOLDSTONE MODE IN CLASSICAL CHIRAL MAGNETS

One of our goals is to derive from a microscopic theory the results one expects based on the simple considerations in Sec. II. As a first step, we show that the phenomenological action for classical helimagnets given by Eq. (2.1) does indeed result in the effective elastic theory given by Eq. (2.5). A derivation from a microscopic quantum mechanical Hamiltonian will be given in Sec. IV.

The classical ϕ^4 theory with a chiral term represented by the action given in Eq. (2.1) can be analyzed in analogy to the action for chiral liquid crystals.[19] In the magnetic case the chiral term with coupling constant c is of the form first proposed by Dzyaloshinski[4] and Moriya,[5] who showed that it is a consequence of the spin-orbit interaction in crystals that lack spatial inversion symmetry.

A. Saddle-point solution

The saddle-point equation $\delta S/\delta M_{\boldsymbol{i}}(\boldsymbol{x}) = 0$ reads

$$[r - a\boldsymbol{\nabla}^2 + c(\boldsymbol{\nabla}\times) + u\boldsymbol{M}^2(\boldsymbol{x})]\boldsymbol{M}(\boldsymbol{x}) = 0, \tag{3.1a}$$

and the free energy density in saddle-point approximation is given by

$$f_{\text{sp}} = \frac{T}{V}S[\boldsymbol{M}_{\text{sp}}], \tag{3.1b}$$

with $\boldsymbol{M}_{\text{sp}}$ a solution of Eq. (3.1a).

The helical field configuration given by Eqs. (2.2) with an amplitude $m_0^2 = -(r + aq^2 - cq)/u$ is a solution for any value of q. The physical value of q is determined from the requirement that the free energy must be minimized, which yields

$$q = c/2a \tag{3.2a}$$

and

$$m_0 = \frac{1}{\sqrt{u}}(c^2/4a - r)^{1/2}. \tag{3.2b}$$

The zero solution $m_0 = 0$ is unstable with respect to the helical solution for all $r < c^2/4a$, and for $c \neq 0$ the ferromagnetic solution $q=0$, $m_0^2 = -r/u$ is always unstable with respect to the helical one since one can always gain energy by making $q \neq 0$ due to the linear momentum dependence of the chiral term $\boldsymbol{M} \cdot (\boldsymbol{\nabla} \times \boldsymbol{M})$.

B. Gaussian fluctuations

1. Disordered phase

In the disordered phase $r > c^2/4a$, the Gaussian propagator is easily found by inverting the quadratic form in Eq. (2.1),

$$\langle M_i(\boldsymbol{k}) M_j(\boldsymbol{p}) \rangle = \delta_{\boldsymbol{k},-\boldsymbol{p}} \frac{1}{(r + aq^2)^2 - c^2 q^2} \times \left[\delta_{ij}(r + aq^2) + \epsilon_{ijl} i c k_l - k_i k_j \frac{c^2}{r + aq^2} \right]. \tag{3.3}$$

The structure of the prefactor in this expression is consistent with the conclusion of Sec. III A: For $r > c^2/4a$, the denominator $N(q) = (r + aq^2)^2 - c^2 q^2$ is minimized by $q = 0$ and $N(q)$ has no zeros in this regime. $N(q)$ first reaches zero at $r = c^2/4a$ and $q = c/2a$, and the disordered phase is unstable for all $r < c^2/4a$. The quantum-critical fluctuations in the disordered phase have been discussed by Schmalian and Turlakov.[24]

2. Ordered phase

In the ordered phase the determination of the Gaussian fluctuations is more complicated. Let us parametrize the order parameter field as follows:

$$\boldsymbol{M}(\boldsymbol{x}) = [m_0 + \delta m(\boldsymbol{x})] \begin{pmatrix} \cos[qz + \phi(\boldsymbol{x})] \\ \sin[qz + \phi(\boldsymbol{x})] \\ \varphi(\boldsymbol{x}) \end{pmatrix}, \tag{3.4a}$$

where $\phi(\boldsymbol{x})$, $\varphi(\boldsymbol{x})$, and $\delta m(\boldsymbol{x})$ describe small fluctuations about the saddle-point solution. Fluctuations of the norm of $\boldsymbol{M}$ one expects to be massive, as they are in the ferromagnetic case, and an explicit calculation confirms this expectation. We thus can keep the norm of $\boldsymbol{M}$ fixed, which means that δm is quadratic in the small fluctuation φ and does not contribute to the Gaussian action. In order to treat the ϕ and φ fluctuations, it is useful to acknowledge that, upon performing a Fourier transform, $\phi(\boldsymbol{k}=0)$ corresponds to taking $\boldsymbol{M}$ at $\boldsymbol{k} = \boldsymbol{q}$, while φ and $\boldsymbol{M}$ come at the same wave number. We therefore write

$$\varphi(\boldsymbol{x}) = \varphi_1(\boldsymbol{x}) \sin qz + \varphi_2(\boldsymbol{x}) \cos qz, \tag{3.4b}$$

where φ_1 and φ_2 are restricted to containing Fourier components with $|\boldsymbol{k}| \ll q$.[25] The Goldstone mode is now expected to be a linear combination of ϕ, φ_1, and φ_2 at zero wave vector. If we expand Eq. (3.4a) to linear order in $\phi \equiv \varphi_0$, substitute this in Eq. (2.1), neglect rapidly fluctuating Fourier components proportional to e^{inqz} with $n \geq 2$, and use the equation of motion (3.1a), we obtain a Gaussian action

$$S^{(2)}[\varphi_i] = \frac{am_0^2}{2} \sum_{\boldsymbol{p}} \sum_{i=0,1,2} \varphi_i(\boldsymbol{p}) \gamma_{ij}(\boldsymbol{p}) \varphi_j(-\boldsymbol{p}), \tag{3.5a}$$

with a matrix

$$\gamma(\boldsymbol{p}) = \begin{pmatrix} \boldsymbol{p}^2 & -iqp_y & -iqp_x \\ iqp_y & q^2 + \boldsymbol{p}^2/2 & iqp_z \\ iqp_x & -iqp_z & q^2 + \boldsymbol{p}^2/2 \end{pmatrix}. \tag{3.5b}$$

The corresponding eigenvalue equation reads

$$(\mu - \boldsymbol{p}^2)(q^2 + \boldsymbol{p}^2/2 - \mu)^2 + q^2 \boldsymbol{p}_\perp^2 (q^2 + \boldsymbol{p}^2/2 - \mu) + q^2 p_z^2 (\boldsymbol{p}^2 - \mu) = 0. \tag{3.6}$$

We see that at $\boldsymbol{p} = 0$ there is one eigenvalue $\mu_1 = 0$ and a doubly degenerate eigenvalue $\mu_{2,3} = q^2$. As expected, there thus is one soft (Goldstone) mode in the ordered phase. The behavior at nonzero wave vector is easily determined by solving Eq. (3.6) perturbatively. The degeneracy of μ_2 and μ_3 is lifted, $\mu_{2,3}(\boldsymbol{p} \to 0) = q^2 \pm qp_z$, and for μ_1 we find

$$\mu_1(\boldsymbol{p} \to 0) = p_z^2 + \boldsymbol{p}_\perp^4/2q^2 + O(p_z^2 \boldsymbol{p}_\perp^2). \tag{3.7a}$$

The corresponding eigenvector is

$$v_1(\boldsymbol{p}) = \phi(\boldsymbol{p}) - i(p_y/q)[1 + O(\boldsymbol{p}_\perp^2)]\varphi_1(\boldsymbol{p}) - i(p_x/q)[1 + O(\boldsymbol{p}_\perp^2)]\varphi_2(\boldsymbol{p}). \tag{3.7b}$$

It has the property

$$\langle v_1(\boldsymbol{p}) v_1(-\boldsymbol{p}) \rangle = 1/am_0^2 \mu_1(\boldsymbol{p}). \tag{3.7c}$$

A comparison with Eq. (2.5) shows that the effective soft-mode action has indeed the form that was expected from the analogy with chiral liquid crystals. If we identify $\sqrt{am_0^2} v_1(\boldsymbol{x})$ with the generalized phase $u(\boldsymbol{x})$, the coupling constants in Eq. (2.5) are $c_z = 1$ and $c_\perp = 1/2$. Repeating the calculation in the presence of a term that breaks the rotational symmetry—e.g., Eq. (2.21)—yields a result consistent with Eq. (2.22) or (2.23), with $b = O(1)$.

IV. NATURE OF THE GOLDSTONE MODE IN QUANTUM CHIRAL MAGNETS

We now turn to the quantum case. Our objective is to develop an effective theory for itinerant helimagnets that is analogous to Hertz's theory for itinerant ferromagnets.[26] That is, starting from a microscopic fermionic action we derive a quantum mechanical generalization of the classical Ginzburg-Landau theory studied in the preceding section. The coefficients of this effective quantum theory will be given in terms of electronic correlation functions, which allows for a semiquantitative analysis of the results. In addition, it provides the building blocks for a treatment of quantum helimagnets by means of many-body perturbation theory, which will allow us to go beyond the treatment at the saddle-point and Gaussian level employed in the present paper. We will show that this theory has a helical ground state given by Eqs. (2.2) and consider fluctuations about this state to find the Goldstone modes.

A. Effective action for an itinerant quantum chiral magnet

Consider a partition function

$$Z = \int D[\bar{\psi},\psi] e^{S[\bar{\psi},\psi]}, \tag{4.1a}$$

given by an electronic action of the form

$$S[\bar{\psi},\psi] = \tilde{S}_0[\bar{\psi},\psi] + S^{\rm t}_{\rm int}. \tag{4.1b}$$

Here $S^{\rm t}_{\rm int}$ describes the spin-triplet interaction. $\tilde{S}_0[\bar{\psi},\psi]$, which we will explicitly specify later, contains all other parts of the action, and the action is a functional of fermionic (i.e., Grassmann-valued) fields ψ and $\bar{\psi}$. The spin-triplet interaction we take to have the form

$$S^{\rm t}_{\rm int} = \frac{1}{2}\int d\boldsymbol{x}d\boldsymbol{y}\int_0^{1/T} d\tau n^i_{\rm s}(\boldsymbol{x},\tau)\boldsymbol{A}_{ij}(\boldsymbol{x}-\boldsymbol{y})n^j_{\rm s}(\boldsymbol{y},\tau). \tag{4.2a}$$

Here and in what follows summation over repeated spin indices is implied. $\boldsymbol{x}$ and $\boldsymbol{y}$ denote the position in real space, τ is the imaginary time variable, and $n^i_{\rm s}(\boldsymbol{x},\tau)$ denote the components of the electronic spin-density field $\boldsymbol{n}_{\rm s}(\boldsymbol{x},\tau)$. The interaction amplitude A is given by

$$A_{ij}(\boldsymbol{x}-\boldsymbol{y}) = \delta_{ij}\Gamma_{\rm t}\delta(\boldsymbol{x}-\boldsymbol{y}) + \epsilon_{ijk}C_k(\boldsymbol{x}-\boldsymbol{y}). \tag{4.2b}$$

The first term, with a pointlike amplitude $\Gamma_{\rm t}$, is the usual Hubbard interaction. The second term involves a cross product $\boldsymbol{n}_{\rm s}(\boldsymbol{x})\times\boldsymbol{n}_{\rm s}(\boldsymbol{y})$ and cannot exist in a homogeneous electron system, which in particular is invariant under spatial inversions. Dzyaloshinski[4] and Moriya[5] have shown that such a term arises from the spin-orbit interaction in lattices that lack inversion symmetry. After coarse graining, it will then also be present in an effective continuum theory valid at length scales large compared to the lattice spacing. In such an effective theory the vector $\boldsymbol{C}(\boldsymbol{x}-\boldsymbol{y})$ is conveniently expanded in powers of gradients. The lowest-order term in the gradient expansion is

$$\boldsymbol{C}(\boldsymbol{x}-\boldsymbol{y}) = c\Gamma_{\rm t}\delta(\boldsymbol{x}-\boldsymbol{y})\,\boldsymbol{\nabla} + O(\nabla^2), \tag{4.2c}$$

with c a constant. The ferromagnetic case[26] can be recovered by putting $c=0$. We now perform a Hubbard-Stratonovich transformation to decouple the spin-triplet interaction. To linear order in the gradients the inverse of the matrix A has the same form as A itself—viz.,

$$A^{-1}_{ij}(\boldsymbol{x}-\boldsymbol{y}) = \delta_{ij}\frac{1}{\Gamma_{\rm t}}\delta(\boldsymbol{x}-\boldsymbol{y}) - \epsilon_{ijk}\frac{c}{\Gamma_{\rm t}}\delta(\boldsymbol{x}-\boldsymbol{y})\partial_k + O(\nabla^2), \tag{4.2d}$$

with $\partial_k = \partial/\partial x_k$ a spatial derivative. The Hubbard-Stratonovich transformation thus produces all of the terms one gets in the ferromagnetic case and, in addition, a term

$$-\frac{1}{2}c\Gamma_{\rm t}\int d\boldsymbol{x}\boldsymbol{M}(\boldsymbol{x},\tau)\cdot[\boldsymbol{\nabla}\times\boldsymbol{M}(\boldsymbol{x},\tau)] + O(\nabla^2), \tag{4.3}$$

where $\boldsymbol{M}$ is the Hubbard-Stratonovich field whose expectation value is proportional to the magnetization. The partition function can then be written in the form

$$\begin{aligned} Z = \int D[\bar{\psi},\psi]e^{\tilde{S}_0[\bar{\psi},\psi]}\int D[\boldsymbol{M}] &\times\exp\left(-(\Gamma_{\rm t}/2)\int dx\boldsymbol{M}(x)\cdot\boldsymbol{M}(x)\right) \\ &\times\exp\left(-c(\Gamma_{\rm t}/2)\int dx\boldsymbol{M}(x)\cdot[\boldsymbol{\nabla}\times\boldsymbol{M}(x)]\right) \\ &\times\exp\left(\Gamma_{\rm t}\int dx\boldsymbol{M}(x)\cdot\boldsymbol{n}_{\rm s}(x)\right). \end{aligned} \tag{4.4}$$

Here we have adopted a four-vector notation $x\equiv(\boldsymbol{x},\tau)$ and $\int dx \equiv \int d\boldsymbol{x}\int_0^{1/T}d\tau$.

Now we consider the ordered phase and write

$$\boldsymbol{M}(x) = \boldsymbol{M}_{\rm sp}(\boldsymbol{x}) + \delta\boldsymbol{M}(x), \tag{4.5}$$

with $\boldsymbol{M}_{\rm sp}$ given by Eq. (2.2b). The parameters m_0 and q which characterize $\boldsymbol{M}_{\rm sp}$ will still have to be determined. By substituting Eq. (4.5) into Eq. (4.4) and formally integrating out the fermions we can write the partition function

$$Z = \int D[\delta\boldsymbol{M}]e^{-\mathcal{A}[\delta\boldsymbol{M}]}, \tag{4.6a}$$

with $\mathcal{A}$ an effective action for the order-parameter fluctuations,

$$\begin{aligned} \mathcal{A}[\delta\boldsymbol{M}] = -\ln Z_0 &+ \frac{\Gamma_{\rm t}}{2}\int dx\boldsymbol{M}(x)\cdot\boldsymbol{M}(x) \\ &+ \frac{c\Gamma_{\rm t}}{2}\int dx\boldsymbol{M}(x)\cdot[\boldsymbol{\nabla}\times\boldsymbol{M}(x)] \\ &- \ln\left\langle \exp\left(\Gamma_{\rm t}\int dx\,\delta\boldsymbol{M}(x)\cdot\boldsymbol{n}_{\rm s}(x)\right)\right\rangle_{S_0}. \end{aligned} \tag{4.6b}$$

Here

$$S_0[\bar{\psi},\psi] = \tilde{S}_0[\bar{\psi},\psi] + \Gamma_{\rm t}\int dx\boldsymbol{M}_{\rm sp}(\boldsymbol{x})\cdot\boldsymbol{n}_{\rm s}(x) \tag{4.7a}$$

is a reference ensemble action for electrons described by $\tilde{S}_0$ in an effective external magnetic field

$$\boldsymbol{H}(\boldsymbol{x}) = \Gamma_{\rm t}\boldsymbol{M}_{\rm sp}(\boldsymbol{x}). \tag{4.7b}$$

Only the Zeeman term due to the effective external field is included in the reference ensemble. Z_0 is the partition function of the reference ensemble,

$$Z_0 = \int D[\bar{\psi},\psi]e^{S_0[\bar{\psi},\psi]}, \tag{4.7c}$$

and $\langle\cdots\rangle_{S_0}$ denotes an average with respect to the action S_0.

The effective action $\mathcal{A}$ can be expanded in a Landau expansion in powers of $\delta\boldsymbol{M}$. To quadratic order this yields

$$\mathcal{A}[\delta\boldsymbol{M}] = \int dx \Gamma_i^{(1)}(x)\,\delta M_i(x) + \frac{1}{2}\int dxdy\,\delta M_i(x)\Gamma_{ij}^{(2)}(x,y)\,\delta M_j(y) + O(\delta M^3), \tag{4.8a}$$

with vertices

$$\Gamma_i^{(1)}(x) = \Gamma_t(1-cq)M_{sp}^i(x) - \Gamma_t\langle n_s^i(x)\rangle_{S_0} \tag{4.8b}$$

and

$$\Gamma_{ij}^{(2)}(x,y) = \delta_{ij}\delta(x-y)\Gamma_t - \epsilon_{ijk}\delta(x-y)\Gamma_t c\partial_k - \chi_0^{ij}(x,y)\Gamma_t^2. \tag{4.8c}$$

Here

$$\chi_0^{ij}(x,y) = \langle n_s^i(x) n_s^j(y)\rangle_{S_0}^c \tag{4.8d}$$

is the spin susceptibility in the reference ensemble. The superscript c in Eq. (4.8d) indicates that only connected diagrams contribute to this correlation function.

B. Properties of the reference ensemble

In order for the formalism developed in the previous subsection to be useful we need to determine the properties of the reference ensemble. As we will see in Sec. IV E and in a forthcoming paper,[12] the reference ensemble is not only necessary for the present formal developments, but also forms the basis for calculating all of the thermodynamic and transport properties of helimagnets. This is because the reference ensemble, rather than just being a useful artifact, has a precise physical interpretation: it incorporates long-range helical order in a fermionic action at a mean-field level.

We first need to specify the action $\tilde{S}_0$. For simplicity, we neglect the spin-singlet interaction contained in $\tilde{S}_0$ and consider free electrons with a Green function

$$G_0(\boldsymbol{k},i\omega_n) = 1/(i\omega_n - \xi_{\boldsymbol{k}}). \tag{4.9a}$$

Here $\omega_n = 2\pi T(n+1/2)$ is a fermionic Matsubara frequency and

$$\xi_{\boldsymbol{k}} = \boldsymbol{k}^2/2m_e - \epsilon_F, \tag{4.9b}$$

with m_e the effective mass of the electrons and ϵ_F the chemical potential or Fermi energy. (Here we neglect spin-orbit interaction effects discussed in Ref. 27 as well as quenched disorder.) For later reference we also define the Fermi wave number $k_F = \sqrt{2m_e\epsilon_F}$, the Fermi velocity $v_F = k_F/m_e$, and the density of states per spin on the Fermi surface, $N_F = k_F m_e/2\pi^2$, in the ensemble $\tilde{S}_0$.

1. Equation of state

The equation of state can be determined from the requirement[28]

$$\langle\delta\boldsymbol{M}(\boldsymbol{x})\rangle = 0, \tag{4.10a}$$

where $\langle\cdots\rangle$ denotes an average with respect to the effective action $\mathcal{A}$. To zero-loop order, this condition reads

$$(1-cq)\boldsymbol{M}_{sp}(\boldsymbol{x}) - \langle\boldsymbol{n}_s(x)\rangle_{S_0} = 0. \tag{4.10b}$$

The zero-loop order or mean-field equation of state is thus determined by the magnetization of the reference ensemble induced by the effective external field $\Gamma_t\boldsymbol{M}_{sp}(\boldsymbol{x})$, Eq. (4.7b). The latter is given by the effective field times a generalized Lindhardt function. The result is

$$1 - cq = -2\Gamma_t\frac{1}{V}\sum_{\boldsymbol{p}} \times T\sum_{i\omega_n}\frac{1}{G_0^{-1}(\boldsymbol{p},i\omega_n)G_0^{-1}(\boldsymbol{p}-\boldsymbol{q},i\omega_n) - \lambda^2}, \tag{4.10c}$$

where $\lambda = m_0\Gamma_t$ is the exchange splitting or Stoner gap. Notice that this provides only one relation between λ and the pitch wave number q. The latter still has to be determined from minimizing the free energy, as in the classical case, Sec. III A.

2. Green function

The basic building block for correlation functions of the reference ensemble is the Green function associated with the action S_0, Eq. (4.7a). With $\tilde{S}_0$ as specified above, the latter reads, explicitly,

$$S_0[\bar{\psi},\psi] = \int dxdy\,\bar{\psi}(x)G^{-1}(x,y)\psi(y), \tag{4.11}$$

with an inverse Green function

$$G^{-1}(x,y) = \left[\left(-\frac{\partial}{\partial\tau} + \frac{1}{2m_e}\boldsymbol{\nabla}^2 + \mu\right)\sigma_0 + \Gamma_t\boldsymbol{M}_{sp}(\boldsymbol{x})\cdot\boldsymbol{\sigma}\right]\delta(x-y). \tag{4.12a}$$

Here $\boldsymbol{\sigma} = (\sigma_1,\sigma_2,\sigma_3)$ denotes the Pauli matrices and σ_0 is the 2×2 unit matrix. Upon Fourier transformation we have

$$G_{\boldsymbol{k},\boldsymbol{p}}^{-1}(i\omega_n) = \delta_{\boldsymbol{k},\boldsymbol{p}}G_0^{-1}(\boldsymbol{k},i\omega_n)\sigma_0 + \Gamma_t\boldsymbol{M}_{sp}(\boldsymbol{k}-\boldsymbol{p})\cdot\boldsymbol{\sigma}. \tag{4.12b}$$

The result of the inversion problem is

$$G_{\boldsymbol{kp}}(i\omega_n) = \delta_{\boldsymbol{kp}}[\sigma_{+-}a_+(\boldsymbol{k},\boldsymbol{q};i\omega_n) + \sigma_{-+}a_-(\boldsymbol{k},\boldsymbol{q};i\omega_n)] + \delta_{\boldsymbol{k}+\boldsymbol{q},\boldsymbol{p}}\sigma_+ b_+(\boldsymbol{k},\boldsymbol{q};i\omega_n) + \delta_{\boldsymbol{k}-\boldsymbol{q},\boldsymbol{p}}\sigma_- b_-(\boldsymbol{k},\boldsymbol{q};i\omega_n), \tag{4.13a}$$

where

$$a_\pm(\boldsymbol{k},\boldsymbol{q};i\omega_n) = \frac{G_0^{-1}(\boldsymbol{k}\pm\boldsymbol{q},i\omega_n)}{G_0^{-1}(\boldsymbol{k},i\omega_n)G_0^{-1}(\boldsymbol{k}\pm\boldsymbol{q},i\omega_n) - \lambda^2}, \tag{4.13b}$$

$$b_{\pm}(\boldsymbol{k},\boldsymbol{q};i\omega_n) = \frac{-\lambda}{G_0^{-1}(\boldsymbol{k},i\omega_n)G_0^{-1}(\boldsymbol{k}\pm\boldsymbol{q},i\omega_n)-\lambda^2}. \tag{4.13c}$$

Here $\sigma_{\pm}=(\sigma_1 \pm i\sigma_2)/2$, $\sigma_{+-}=\sigma_+\sigma_-$, and $\sigma_{-+}=\sigma_-\sigma_+$.

3. Spin susceptibility

Since the reference ensemble describes noninteracting electrons, the reference ensemble spin susceptibility factorizes into a product of two Green functions. Applying Wick's theorem to Eq. (4.8d) one obtains

$$\chi_0^{ij}(x,y) = -\,\mathrm{tr}[\sigma_i G(x,y)\sigma_j G(y,x)] \tag{4.14a}$$

or, after a Fourier transform,

$$\chi_0^{ij}(\boldsymbol{k},\boldsymbol{p};i\Omega_n) = \frac{-1}{V}\sum_{\boldsymbol{k}',\boldsymbol{p}'} T\sum_{i\omega_n} \mathrm{tr}[\sigma_i G_{\boldsymbol{k}',\boldsymbol{p}'}(i\omega_n)\times\sigma_j G_{\boldsymbol{p}'+\boldsymbol{p},\boldsymbol{k}'+\boldsymbol{k}}(i\omega_n + i\Omega_n)]. \tag{4.14b}$$

Here the trace is over the spin degrees of freedom and $\Omega_n = 2\pi T n$ is a bosonic Matsubara frequency.

From the structure of the Green function, Eq. (4.13a), it is obvious that χ_0 is nonzero if $\boldsymbol{k}$ and $\boldsymbol{p}$ differ by zero, $\pm\boldsymbol{q}$, or $\pm 2\boldsymbol{q}$. The full expression in terms of $a_{\pm}$ and $b_{\pm}$ is lengthy and given in Appendix B.

4. Ferromagnetic limit

It is illustrative to check the ferromagnetic limit $\boldsymbol{q}\to 0$ at this point. In this case $\boldsymbol{M}_{\mathrm{sp}}=(m_0,0,0)$ becomes position independent and both the Green function and the reference ensemble spin susceptibility become diagonal in momentum space. For zero momentum and frequency, the latter is also diagonal in spin space,

$$\chi_{0,\boldsymbol{q}=0}^{ij}(\boldsymbol{k},\boldsymbol{p};i\Omega_n) = \delta_{\boldsymbol{k},\boldsymbol{p}}\chi_{0,\boldsymbol{q}=0}^{ij}(\boldsymbol{k},i\Omega_n), \tag{4.15a}$$

$$\chi_{0,\boldsymbol{q}=0}^{ij}(0,i0) = \delta_{ij}[\delta_{i1}\chi_{\mathrm{L}} + (1-\delta_{i1})\chi_{\mathrm{T}}]. \tag{4.15b}$$

The static and homogeneous transverse susceptibility χ_{T} of the reference ensemble is related to the magnetization by a Ward identity[28,29] [remember that $\Gamma_{\mathrm{t}}\boldsymbol{M}_{\mathrm{sp}}$ is the effective field in the reference ensemble; see Eq. (4.7b)]

$$\langle \boldsymbol{n}_{\mathrm{s}}(x)\rangle_0 = \Gamma_{\mathrm{t}}\boldsymbol{M}_{\mathrm{sp}}\chi_{\mathrm{T}}. \tag{4.16}$$

A calculation of χ_{T} by evaluating Eq. (4.14b) for $\boldsymbol{q}=0$ shows that Eq. (4.16) is the equation of state, Eq. (4.10c), for $\boldsymbol{q}=0$. Equation (4.10c) thus represents the generalization of this Ward identity to the helimagnetic case.

C. Gaussian fluctuations I: $\boldsymbol{k}=\boldsymbol{q}$ modes

We are now in a position to explicitly write down the fluctuation action given by Eqs. (4.8). From both the phenomenological arguments in Sec. II A and the classical field theory in Sec. III A we expect the static behavior to be correctly described by the fluctuations with wave numbers close to the pitch wave number q, while Sec. II B suggests that treating the dynamics correctly requires one to also take into account fluctuations with wave numbers near zero. For the sake of transparency we first concentrate on the $\boldsymbol{k}=\boldsymbol{q}$ modes. We will later expand our set of modes to study the effects of the $\boldsymbol{k}=0$ modes on the dynamics.

1. Gaussian action

We parametrize the fluctuations of the order parameter as in the classical case, Eqs. (3.4), but now allow for the fields ϕ, φ_1, and φ_2 to depend on imaginary time or Matsubara frequency. To linear order in the fluctuations we have

$$\delta\boldsymbol{M}(x) = m_0\begin{pmatrix} -\phi(x)\sin(\boldsymbol{q}\cdot\boldsymbol{x}) \\ \phi(x)\cos(\boldsymbol{q}\cdot\boldsymbol{x}) \\ \varphi_1(x)\sin(\boldsymbol{q}\cdot\boldsymbol{x}) + \varphi_2(x)\cos(\boldsymbol{q}\cdot\boldsymbol{x}) \end{pmatrix}. \tag{4.17}$$

As in the classical case we have anticipated that fluctuations of the norm of the order parameter are massive. The term linear in $\delta\boldsymbol{M}$ vanishes due to the saddle-point condition, and the Gaussian term can be expressed in terms of integrals by using Eqs. (4.14b), (B1), and (B2). Using the notation $\phi(x)\equiv\varphi_0(x)$ as in the classical case, we find a Gaussian action[30]

$$\mathcal{A}^{(2)}[\varphi_i] = \frac{\lambda^2}{2}\sum_{\boldsymbol{p}}\sum_{i\Omega_n}\sum_{i=0,1,2}\varphi_i(\boldsymbol{p},i\Omega_n)\,\gamma_{ij}^{(\boldsymbol{q})}(\boldsymbol{p},i\Omega_n)\times\varphi_j(-\boldsymbol{p},-i\Omega_n). \tag{4.18a}$$

Here the matrix $\gamma^{(\boldsymbol{q})}$ is the quantum mechanical analog of Eq. (3.5b), which couples the phase or $\boldsymbol{k}=\boldsymbol{q}$ modes among each other. In a four-vector notation $k\equiv(\boldsymbol{k},i\Omega_n)\equiv(k_x,k_y,k_z,i\Omega_n)$ it is given by

$$\gamma^{(\boldsymbol{q})}(k) = \begin{pmatrix} (1-cq)/\Gamma_{\mathrm{t}} - f_{\phi\phi}(k) & -ick_y/2\Gamma_{\mathrm{t}} & -ick_x/2\Gamma_{\mathrm{t}} \\ ick_y/2\Gamma_{\mathrm{t}} & 1/2\Gamma_{\mathrm{t}} - f_{11}(k) & -f_{12}(k) \\ ick_x/2\Gamma_{\mathrm{t}} & f_{12}(k) & 1/2\Gamma_{\mathrm{t}} - f_{11}(k) \end{pmatrix}. \tag{4.18b}$$

Here

$$f_{\phi\phi}(k) = \varphi_{\phi\phi}(k) + \varphi_{\phi\phi}(-k), \tag{4.18c}$$

$$f_{11}(k) = \varphi_{11}(k) + \varphi_{11}(-k), \tag{4.18d}$$

$$f_{12}(k) = i[\varphi_{11}(k) - \varphi_{11}(-k)], \tag{4.18e}$$

where

$$\varphi_{\phi\phi}(k) = -\int_p \frac{G_0^{-1}(\boldsymbol{p}-\boldsymbol{k},i\omega_m - i\Omega_n)G_0^{-1}(\boldsymbol{p}-\boldsymbol{q},i\omega_m) - \lambda^2}{[G_0^{-1}(\boldsymbol{p}-\boldsymbol{k},i\omega_m - i\Omega_n)G_0^{-1}(\boldsymbol{p}-\boldsymbol{k}-\boldsymbol{q},i\omega_m - i\Omega_n) - \lambda^2][G_0^{-1}(\boldsymbol{p},i\omega_m)G_0^{-1}(\boldsymbol{p}-\boldsymbol{q},i\omega_m) - \lambda^2]}, \tag{4.18f}$$

$$\varphi_{11}(k) = -\int_p \frac{G_0^{-1}(\boldsymbol{p}-\boldsymbol{k},i\omega_m - i\Omega_n)G_0^{-1}(\boldsymbol{p}+\boldsymbol{q},i\omega_m) + G_0^{-1}(\boldsymbol{p}-\boldsymbol{k}-\boldsymbol{q},i\omega_m - i\Omega_n)G_0^{-1}(\boldsymbol{p},i\omega_m) - 2\lambda^2}{[G_0^{-1}(\boldsymbol{p}-\boldsymbol{k},i\omega_m - i\Omega_n)G_0^{-1}(\boldsymbol{p}-\boldsymbol{k}-\boldsymbol{q},i\omega_m - i\Omega_n) - \lambda^2][G_0^{-1}(\boldsymbol{p},i\omega_m)G_0^{-1}(\boldsymbol{p}+\boldsymbol{q},i\omega_m) - \lambda^2]}, \tag{4.18g}$$

with $\int_p \equiv (1/V)\Sigma_{\boldsymbol{p}} T \Sigma_{i\omega_m}$.

In contrast to the classical case, here it is not obvious that the Gaussian vertex, Eq. (4.18b), has a zero eigenvalue. To see that it does, we invoke the equation of state (4.10c). By comparing this with Eqs. (4.18c) and (4.18f), we see that

$$1 - cq - \Gamma_t f_{\phi\phi}(0,i0) = 0. \tag{4.19a}$$

Similarly,

$$1/2 - \Gamma_t f_{11}(0,i0) = cq/2\Gamma_t. \tag{4.19b}$$

Since $c \propto q$ [see Eqs. (3.2a) and (4.21) below], it follows that the quantum mechanical vertex $\gamma^{(\mathbf{q})}(\mathbf{p},i\Omega_n)$ has the same structure as its classical counterpart, Eq. (3.5b), except for an additional frequency dependence in the quantum mechanical case.

To determine the eigenvalues we need to evaluate the integrals to lowest nontrivial order in the wave vector and the frequency. A complete calculation is rather difficult, and we restrict ourselves to the limit $\lambda \gg qv_F$. The calculation, the details of which we relegate to Appendix C, yields

$$f_{\phi\phi}(\boldsymbol{k},i\Omega_n) = f_{\phi\phi}(0,i0) - 2N_F\left[\alpha\left(\frac{\boldsymbol{k}}{2k_F}\right)^2 - \beta\left(\frac{i\Omega_n}{4\epsilon_F}\right)^2 + \gamma_\phi \frac{|\Omega_n|}{4\epsilon_F}\frac{k_z^2}{2k_F|\boldsymbol{k}|}\right], \tag{4.20a}$$

$$f_{11}(\boldsymbol{k},i\Omega_n) = f_{11}(0,i0) - N_F\left[\alpha\left(\frac{\boldsymbol{k}}{2k_F}\right)^2 - \beta\left(\frac{i\Omega_n}{4\epsilon_F}\right)^2 + \gamma_1\frac{|\Omega_n|}{4\epsilon_F}\frac{\boldsymbol{k}_\perp^2}{(2k_F)^2}\right], \tag{4.20b}$$

$$f_{12}(\boldsymbol{k},i\Omega_n) = -i2N_F\alpha\frac{qk_z}{(2k_F)^2}. \tag{4.20c}$$

Here

$$\alpha = 1/3, \tag{4.20d}$$

$$\beta = 4\epsilon_F^2/\lambda^2, \tag{4.20e}$$

$$\gamma_\phi = \pi(qv_F)^2/8\lambda^2, \tag{4.20f}$$

$$\gamma_1 = -4\gamma_\phi(k_F/q)^3. \tag{4.20g}$$

These expressions are valid for $|\Omega_n| \ll \lambda \ll \epsilon_F$, $|\boldsymbol{k}| \ll q \ll k_F$, and $qv_F \ll \lambda$. The damping terms have the form shown if, in addition, $|\Omega| \ll v_F|\boldsymbol{k}|$.

We now also can express the pitch wave number q in terms of the parameters of our model. The minimization of the saddle-point free energy proceeds as in the classical case, and by comparing Eq. (3.2a) with Eqs. (4.17), (4.18a), (4.18b), (4.19a), and (4.20a), we find

$$q = ck_F^2/N_F\Gamma_t\alpha. \tag{4.21}$$

2. Eigenvalue problem

The diagonalization of the matrix $\gamma^{(\boldsymbol{q})}$, Eq. (4.18b), can be done perturbatively as in the classical case. The soft (Goldstone) mode—i.e., the eigenvector corresponding to the smallest eigenvalue—is

$$v(\boldsymbol{k},i\Omega_n) = \phi(\boldsymbol{k},i\Omega_n) - i(k_y/q)[1 + O(\boldsymbol{k}_\perp^2)]\varphi_1(\boldsymbol{k},i\Omega_n) - i(k_x/q)[1 + O(\boldsymbol{k}_\perp^2)]\varphi_2(\boldsymbol{k},i\Omega_n). \tag{4.22}$$

The helimagnon is proportional to the v-v-correlation function, which in turn is proportional to the inverse of the smallest eigenvalue of the matrix $\gamma^{(\boldsymbol{q})}$. With $\boldsymbol{\kappa} = \sqrt{\alpha}\boldsymbol{k}/2k_F$, $\boldsymbol{Q} = \sqrt{\alpha}\boldsymbol{q}/2k_F$, $\omega = \sqrt{\beta}\Omega_n/4\epsilon_F \equiv \Omega_n/2\lambda$, $c_\phi = \gamma_\phi/\sqrt{\alpha\beta}$, and $c_1 = \gamma_1/\alpha\sqrt{\beta}$, the latter reads

$$\gamma^{(q)}(k) = 2N_{\mathrm{F}}\begin{pmatrix} \kappa^2+\omega^2+c_\phi|\omega|\kappa_z^2/|\boldsymbol{\kappa}| & -iQ\kappa_y & -iQ\kappa_x \\ iQ\kappa_y & Q^2+\frac{1}{2}\kappa^2+\frac{1}{2}\omega^2-\frac{1}{2}c_1|\omega|\boldsymbol{\kappa}_\perp^2 & iQ\kappa_z \\ iQ\kappa_x & -iQ\kappa_z & Q^2+\frac{1}{2}\kappa^2+\frac{1}{2}\omega^2-\frac{1}{2}c_1|\omega|\boldsymbol{\kappa}_\perp^2 \end{pmatrix}. \tag{4.23}$$

The eigenvalue equation, which is the quantum mechanical generalization of Eq. (3.6), can be simplified if we anticipate, from Secs. II and III B, that the smallest eigenvalue scales as $\mu \sim \kappa_z^2 \sim \boldsymbol{\kappa}_\perp^4 \sim \omega^2$. Keeping only terms up to $O(\kappa_z^2)$, the eigenvalue equation reads

$$\left(\mu-\kappa^2-\omega^2-c_\phi|\omega|\frac{\kappa_z^2}{|\boldsymbol{\kappa}|}\right)Q^4+Q^2\boldsymbol{\kappa}_\perp^2\left(Q^2+\frac{\boldsymbol{\kappa}_\perp^2}{2}\right)=0. \tag{4.24}$$

This result has several interesting aspects, which will be very useful when we generalize the theory to include the $\boldsymbol{k}=0$ modes in Sec. IV D. First, of the function f_{11}, Eq. (4.20b), only the constant and the term proportional to $\boldsymbol{k}_\perp^2 \sim k_z$ contribute to the leading terms in the eigenvalue. In particular, the damping term proportional to γ_1, which has a potential to lead to an overdamping of the Goldstone mode, does not contribute. Second, the function f_{12}, which describes the coupling between the phase modes φ_1 and φ_2, does not contribute to the leading result. Indeed, the only role of φ_1 and φ_2 is to subtract the $\boldsymbol{\kappa}_\perp^2$ contribution from the eigenvalue, and this is accomplished entirely by the purely static matrix elements in Eq. (4.18b) which do not depend on reference ensemble correlation functions.

For the smallest eigenvalue we find, from Eq. (4.24),

$$\mu(\boldsymbol{\kappa}\to 0,\omega\to 0)=\kappa_z^2+\omega^2+\frac{\boldsymbol{\kappa}_\perp^4}{2Q^2}+c_\phi|\omega|\frac{\kappa_z^2}{|\boldsymbol{\kappa}|}+O(\kappa_z^3). \tag{4.25}$$

Since the Goldstone correlation function is proportional to the inverse of the smallest eigenvalue, this result has indeed the functional form we expect from the phenomenological treatment in Sec. II; see Eqs. (2.18a) and (2.19a). At zero frequency it also is consistent with the result of the classical field theory in Sec. III. However, in contrast to Eq. (2.13) the mass of the zero-wave-number mode does not enter in Eq. (4.25), which suggests that the frequency scale is not correctly described yet. This was to be expected; see the remarks at the start of Sec. IV C. We will see in Sec. IV D that the $\boldsymbol{k}=0$ mode has to be included in the analysis to obtain the correct prefactor of the ω^2 term in the smallest eigenvalue, in agreement with the phenomenological analysis.

3. Ferromagnetic limit

Before we expand our set of modes it is again illustrative to consider the ferromagnetic limit $\boldsymbol{q}=0$. Going back to Eqs. (4.17), we see that in this limit φ_1 disappears and ϕ and φ_2 play the roles of the two independent field components π_1 and π_2 in a ferromagnetic nonlinear σ model, which are both soft.[31] The Gaussian action is given by the reference ensemble spin susceptibility at $\boldsymbol{q}=0$, and one finds[32]

$$\mathcal{A}^{(2)}[\phi,\varphi_2]=\frac{1}{2}N_{\mathrm{F}}\Gamma_{\mathrm{t}}^2\sum_{\boldsymbol{p},i\Omega_n}\sum_{i=1,2}\pi_i(\boldsymbol{p},i\Omega_n)\tilde{\gamma}_{ij}(\boldsymbol{p},i\Omega_n)\times\pi_j(-\boldsymbol{p},-i\Omega_n), \tag{4.26}$$

with $\pi_1\equiv\phi$ and $\pi_2\equiv\varphi_2$ and a matrix

$$\tilde{\gamma}_{ij}(\boldsymbol{p},i\Omega_n)=\begin{pmatrix}\kappa^2 & 2i(i\omega)\\ -2i(i\omega) & \kappa^2\end{pmatrix}. \tag{4.27}$$

Comparing with the eigenvalue problem given by Eq. (4.23) we see that the latter does *not* correctly reproduce the ferromagnetic result upon dropping φ_1 and letting $\boldsymbol{q}\to 0$. This is not surprising, since the gradient expansion implicit in the effective field theory approach implies that we are restricted to wave numbers small compared to q. That is, the validity of Eq. (4.23) shrinks to zero as $\boldsymbol{q}\to 0$. However, it raises the following question. The leading frequency dependence of the ferromagnetic magnon is determined by the off-diagonal elements of the matrix $\tilde{\gamma}$. Similarly, the time-dependent Ginzburg-Landau theory of Sec. II B suggests that the leading frequency dependence of the helimagnon is produced by the coupling of the phase mode to the homogeneous magnetization. Although the latter is massive at wave number q, its conserved character makes it important for the dynamics. In contrast, in the treatment above the leading frequency dependence was produced by the phase correlation functions. We therefore extend our set of modes to allow for a coupling between the phase modes, which represent $\boldsymbol{k}=\boldsymbol{q}$ fluctuations of the magnetization, and the homogeneous magnetization.

D. Gaussian fluctuations II: Coupling between $k=q$ modes and $k=0$ modes

The discussion in the preceding subsection suggests to generalize the expression for the magnetization fluctuations, Eq. (4.17), by writing

$$\delta\boldsymbol{M}(x)=m_0\begin{pmatrix}-\phi(x)\sin(\boldsymbol{q}\cdot\boldsymbol{x})\\ \phi(x)\cos(\boldsymbol{q}\cdot\boldsymbol{x})+\pi_2(x)\\ \varphi_1(x)\sin(\boldsymbol{q}\cdot\boldsymbol{x})+\varphi_2(x)\cos(\boldsymbol{q}\cdot\boldsymbol{x})+\pi_1(x)\end{pmatrix}. \tag{4.28}$$

That is, we add the $\boldsymbol{k}=0$ fluctuations to the $\boldsymbol{k}=\boldsymbol{q}$ fluctuations.[33]

1. Gaussian action

If one repeats the development of the previous subsection for the current set of five modes, one finds that of the two $\boldsymbol{k}=0$ modes only π_1 contributes to the leading terms in the eigenvalue problem. π_2 does not couple to ϕ, and its couplings to φ_1 and φ_2 produce only higher-order corrections. π_1, on the other hand, couples to ϕ in a way that preserves the off-diagonal frequency terms characteristic for the ferromagnetic problem [see Eq. (4.27)] and needs to be kept. These observations are in agreement with the phenomenological theory of Sec. II B, where only the three-component of the homogeneous magnetization is coupled to the phase mode. They also are consistent with the observation in Sec. IV C 2 that φ_1 and φ_2 serve only to provide the correct static structure of the theory. We thus drop π_2 and consider the 4×4 problem given by the phase modes plus π_1.

The Gaussian action that generalizes Eqs. (4.18) now reads

$$\mathcal{A}^{(2)}[\varphi_i] = \frac{\lambda^2}{2}\sum_{\boldsymbol{p}}\sum_{i\Omega_n}\sum_{i=0}^{3}\varphi_i(\boldsymbol{p},i\Omega_n)\,\gamma_{ij}^{(\boldsymbol{q},0)}(\boldsymbol{p},i\Omega_n)\times\varphi_j(-\boldsymbol{p},-i\Omega_n). \tag{4.29a}$$

Here $\varphi_3\equiv\pi_1$ and the matrix $\gamma^{(\boldsymbol{q},0)}$, which couples the phase modes to π_1, reads, in a block matrix notation,

$$\gamma^{(\boldsymbol{q},0)}(k) = \begin{pmatrix} & & & -ih_{\phi 1}(k) \\ & \gamma^{(\boldsymbol{q})}(k) & & 0 \\ & & & 0 \\ ih_{\phi 1}(k) & 0 & 0 & 1/\Gamma_{\rm t} - g_{11}(k)\end{pmatrix}, \tag{4.29b}$$

with $\gamma^{(\boldsymbol{q})}$ from Eq. (4.18b). In addition to the functions defined in Eqs. (4.18), we need

$$g_{11}(\boldsymbol{k},i\Omega_n) = 4\varphi_{11}(\boldsymbol{k}-\boldsymbol{q},i\Omega_n), \tag{4.29c}$$

with φ_{11} from Eq. (4.18g), and

$$h_{\phi 1}(\boldsymbol{k},i\Omega_n) = \eta_{\phi 1}(\boldsymbol{k},i\Omega_n) - \eta_{\phi 1}(-\boldsymbol{k},-i\Omega_n), \tag{4.29d}$$

where

$$\eta_{\phi 1}(k) = \lambda\int_p \frac{G_0^{-1}(\boldsymbol{p}-\boldsymbol{k},i\omega_m-i\Omega_n) - G_0^{-1}(\boldsymbol{p}-\boldsymbol{q},i\omega_m)}{[G_0^{-1}(\boldsymbol{p}-\boldsymbol{k},i\omega_m-i\Omega_n)G_0^{-1}(\boldsymbol{p}-\boldsymbol{k}-\boldsymbol{q},i\omega_m-i\Omega_n)-\lambda^2][G_0^{-1}(\boldsymbol{p},i\omega_m)G_0^{-1}(\boldsymbol{p}-\boldsymbol{q},i\omega_m)-\lambda^2]}. \tag{4.29e}$$

Performing these integrals in the limit $\lambda \gg q v_{\rm F}$ yields the leading contributions (see Appendix C)

$$g_{11}(\boldsymbol{k},i\Omega_n) = 1/\Gamma_{\rm t} - 2N_{\rm F}\left[\alpha\left(\frac{\boldsymbol{q}}{2k_{\rm F}}\right)^2 + \alpha\left(\frac{\boldsymbol{k}}{2k_{\rm F}}\right)^2 + \beta\left(\frac{i\Omega_n}{4\epsilon_{\rm F}}\right)^2 - \frac{1}{2}\gamma_\phi\frac{|\Omega_n|}{4\epsilon_{\rm F}}\frac{2k_{\rm F}\boldsymbol{k}_\perp^2}{|\boldsymbol{k}|^3}\right], \tag{4.30a}$$

$$h_{\phi 1}(\boldsymbol{k},i\Omega_n) = 2N_{\rm F}8\sqrt{\beta}\frac{i\Omega_n}{4\epsilon_{\rm F}}. \tag{4.30b}$$

2. Eigenvalue problem

Now consider the generalization of Eq. (4.23). It is obvious from Eqs. (4.29b) and (4.30) that the mode π_1 will contribute to the eigenvalue a term proportional to Ω^2 whose prefactor is large compared to the one in Eq. (4.25) by a factor of $(k_{\rm F}/q)^2$. This is because the mass of π_1 is proportional to $(q/k_{\rm F})^2$. Consequently, one can neglect the terms proportional to ω^2 in the diagonal elements of $\gamma^{(\boldsymbol{q})}$, Eq. (4.23). The leading damping term, however, is still given by $f_{\phi\phi}$, Eq. (4.20a). Dropping all terms that yield contributions of higher order than k_z^2 in the eigenvalue equation, the matrix $\gamma^{(\boldsymbol{q},0)}$, Eq. (4.29b), reads, in the notation of Sec. IV C 2,

$$\gamma^{(\boldsymbol{q},0)}(k) = 2N_{\rm F}\begin{pmatrix} \kappa^2 + c_\phi|\omega|\dfrac{\kappa_z^2}{|\boldsymbol{\kappa}|} & -iQ\kappa_y & -iQ\kappa_x & -8i(i\omega) \\ iQ\kappa_y & Q^2+\dfrac{1}{2}\boldsymbol{\kappa}_\perp^2 & iQ\kappa_z & 0 \\ iQ\kappa_x & -iQ\kappa_z & Q^2+\dfrac{1}{2}\boldsymbol{\kappa}_\perp^2 & 0 \\ 8i(i\omega) & 0 & 0 & Q^2 \end{pmatrix}. \tag{4.31}$$

The smallest eigenvalue is

$$\mu(\boldsymbol{\kappa} \to 0, \omega \to 0) = \kappa_z^2 + 64\frac{\omega^2}{Q^2} + \frac{\boldsymbol{\kappa}_\perp^4}{2Q^2} + c_\phi|\omega|\frac{\kappa_z^2}{|\boldsymbol{\kappa}|} + O(\kappa_z^3), \tag{4.32a}$$

and the corresponding eigenvector reads

$$v(\boldsymbol{k}, i\Omega_n) = \phi(\boldsymbol{k}, i\Omega_n) - i(\kappa_y/Q)\varphi_1(\boldsymbol{k}, i\Omega_n) - i(\kappa_x/Q)\varphi_2(\boldsymbol{k}, i\Omega_n) + (4\omega/Q^2)\pi_1(\boldsymbol{k}, i\Omega_n). \tag{4.32b}$$

Notice that the origin of the leading frequency dependence is consistent with the ferromagnetic limit, Eq. (4.27), and, more importantly, with the time-dependent Ginzburg-Landau theory in Sec. II B. Namely, it is produced by the coupling of the three-component of the $\boldsymbol{k}=0$ magnetization fluctuation to the phase mode at $\boldsymbol{k}=\boldsymbol{q}$. The frequency dependence in Eq. (4.23), on the other hand, corresponded to second-order time derivative corrections to the kinetic equation (2.6).

E. Goldstone mode and the spin susceptibility

1. Goldstone mode in the clean limit

We are now in a position to determine the Goldstone mode. Defining the latter as $g(\boldsymbol{k}, i\Omega_n) = (\sqrt{2N_F}\sqrt{192k_F/q})v(\boldsymbol{k}, i\Omega_n)$ and returning to ordinary units, we find, from Eqs. (4.32),

$$\langle g(\boldsymbol{k}, i\Omega_n)g(-\boldsymbol{k}, -i\Omega_n)\rangle = \frac{1}{-(i\Omega_n)^2 + \omega_0^2(\boldsymbol{k}) + |\Omega_n|\gamma(\boldsymbol{k})}, \tag{4.33a}$$

where

$$\omega_0(\boldsymbol{k}) = \lambda\frac{q}{24k_F}\sqrt{\frac{1}{3}k_z^2/(2k_F)^2 + \frac{1}{6}\boldsymbol{k}_\perp^4/(2qk_F)^2} \tag{4.33b}$$

and

$$\gamma(\boldsymbol{k}) = \frac{\pi}{96}\epsilon_F\frac{q^4}{(2k_F)^4}\frac{k_z^2}{2k_F|\boldsymbol{k}|}. \tag{4.33c}$$

This has the same functional form as the result of the phenomenological treatment in Sec. II; see Eqs. (2.18a) and (2.19a). The current microscopic derivation reveals in addition that the prefactor of the damping coefficient is smaller than that of the resonance frequency by at least a factor of $(qv_F/\lambda)(q/k_F)$. The Goldstone mode is thus propagating and weakly damped for all orientations of the wave vector.[34] As in the classical case, adding cubic anisotropic terms—e.g., the quantum mechanical generalization of Eq. (2.21)—leads to a soft-mode energy of the form of Eq. (2.23).

2. Goldstone mode in the presence of quenched disorder

Equation (4.33c) holds for clean systems. As we have mentioned in the context of Eqs. (2.19), the structure of the damping term is expected to change qualitatively in the presence of even weak impurity scattering. Let $\tau_{\rm imp}$ be the inelastic scattering rate due to quenched impurities. Then the bare Green function G_0, Eq. (4.9a), acquires a finite lifetime,[35]

$$G_0(\boldsymbol{k}, i\omega_n) = 1/[i\omega_n - \xi_{\boldsymbol{k}} + (i/2\tau_{\rm imp})\text{sgn}\ \omega_n]. \tag{4.34}$$

For weak disorder $\epsilon_F\tau_{\rm imp} \gg 1$, the leading effect is that the hydrodynamic singularity in the generalized Lindhard function $\phi^{(2)}_{\phi\phi}$, Eq. (C1f), is now protected. The net effect is the replacement $1/v_F|\boldsymbol{k}| \to \tau_{\rm imp}$ in the damping term in $f_{\phi\phi}$, Eq. (4.20a), and hence in the damping coefficient $\gamma(\boldsymbol{k})$. The Goldstone mode is then given by Eq. (4.33a), with the resonance frequency still given by Eq. (4.33b) and

$$\gamma(\boldsymbol{k}) = \frac{\pi}{24}\epsilon_F(\epsilon_F\tau_{\rm imp})\frac{q^4}{(2k_F)^4}\frac{k_z^2}{(2k_F)^2}. \tag{4.35}$$

This is again consistent with the result of the phenomenological treatment in Sec. II; see Eq. (2.19b). Since $\gamma(\boldsymbol{k}) \sim k_z^2 \ll \omega_0(\boldsymbol{k}) \sim k_z$, the mode is again propagating.

3. Physical spin susceptibility

The helimagnon correlation function is simply related to the physical susceptibility, which is directly measurable by inelastic neutron scattering.[36–38] To express the latter in terms of order-parameter correlation functions we generalize the partition function, Eq. (4.1a), to a generating functional for spin-density correlation functions,

$$Z[\boldsymbol{j}] = \int D[\bar{\psi}, \psi]\exp\left(S[\bar{\psi}, \psi] + \int dx\boldsymbol{j}(x)\cdot\boldsymbol{n}_s(x)\right), \tag{4.36}$$

where $\boldsymbol{j}(x)$ is a source field. The spin susceptibility is given by

$$\begin{aligned}\chi_s^{ij}(x,y) &= \langle n_s^i(x)n_s^j(y)\rangle_S - \langle n_s^i(x)\rangle_S\langle n_s^j(y)\rangle_S \\ &= \left.\frac{\delta^2}{\delta j_i(x)\delta j_j(y)}\right|_{\boldsymbol{j}=0}\ln Z[\boldsymbol{j}] \\ &= \Gamma_t^2\langle(A^{-1}\delta M)_i(x)(A^{-1}\delta M)_j(y)\rangle_{\mathcal{A}}.\end{aligned} \tag{4.37}$$

Here A^{-1} is the matrix given in Eq. (4.2d) and the last average is to be taken with respect to the effective action $\mathcal{A}$, Eqs. (4.8).

The chiral nature of the helix is also reflected in the spin fluctuations and will become manifest if the spin susceptibility is measured with circularly polarized neutrons. To see this, it is useful to define magnetization fluctuations $\delta M_\pm = \delta M_1 \pm i\delta M_2$. Similarly, we define gradient operators $\partial_\pm = \partial_x \pm i\partial_y$. With these definitions one finds

$$\Gamma_t(A^{-1}\delta M)_\pm(x) = \delta M_\pm(x) \pm ic\partial_z\delta M_\pm(x) \mp ic\partial_\pm\delta M_z(x), \tag{4.38a}$$

$$\Gamma_t(A^{-1}\delta M)_z(x) = \delta M_z(x) + i\frac{c}{2}[\partial_+\delta M_-(x) - \partial_-\delta M_+(x)]. \tag{4.38b}$$

By means of Eq. (4.28) we can express the components of $\delta\boldsymbol{M}$ in terms of $\varphi_0 \equiv \phi$, φ_1, φ_2, and $\varphi_3 \equiv \pi_1$,

$$\delta M_\pm(x) = \pm i m_0 \phi(x) e^{\pm i\boldsymbol{q}\cdot\boldsymbol{x}}, \tag{4.39a}$$

$$\delta M_z(x) = m_0\pi_1(x) + \frac{m_0}{2}[(\varphi_2(x) - i\varphi_1(x))e^{\pm i\boldsymbol{q}\cdot\boldsymbol{x}} + \text{c.c.}], \tag{4.39b}$$

where c.c. denotes the complex conjugate of the preceding expression. The elements of the susceptibility tensor can therefore be expressed in terms of the correlation functions of the φ_i, which we denote by $\chi_{\phi\phi}$, etc. The various correlation functions can be determined from the Gaussian action $\mathcal{A}^{(2)}$, Eq. (4.29a), with the vertex function $\gamma^{(\boldsymbol{q},0)}$ given by Eq. (4.31). The inverse of the latter matrix reads

$$[\gamma^{(2)}(\boldsymbol{p},i\Omega_n)]^{-1} = \frac{Q^3}{2N_F\mu(\boldsymbol{p},i\Omega_n)}\begin{pmatrix} Q^3 & iQ^2\kappa_y - Q^4\kappa_z\kappa_x & iQ^2\kappa_x + Q^4\kappa_z\kappa_y & -8Q\omega + O(\omega^2) \\ -iQ^2\kappa_y - Q^4\kappa_z\kappa_x & -Q\kappa_x^2 & Q\kappa_x\kappa_y & 4i\omega\kappa_y \\ -iQ^2\kappa_x + Q^4\kappa_z\kappa_y & Q\kappa_x\kappa_y & -Q\kappa_y^2 & 4i\omega\kappa_x \\ 8Q\omega & 4i\omega\kappa_y & 4i\omega\kappa_x & Q\kappa_z^2 + Qc_\phi|\omega|\kappa_z^2/|\boldsymbol{\kappa}| \end{pmatrix}. \tag{4.40}$$

Here we use the same notation as is Eqs. (4.23) and (4.31), and corrections to each matrix element are one power higher in $\kappa_z \sim \boldsymbol{\kappa}_\perp^2 \sim \omega$ than the terms shown. All of the correlation functions that determine the spin susceptibility are proportional to the inverse of the smallest eigenvalue μ, Eq. (4.32a), which scales as ω^2. $\langle\phi\phi\rangle$ is the softest; it scales as $1/\omega^2$. The autocorrelation functions of ϕ_1 and ϕ_2 have an additional factor of $\boldsymbol{\kappa}_\perp^2 \sim \omega$ in the numerator and thus scale as $1/\omega$, and so does $\langle\phi_1\phi_2\rangle$. The autocorrelation function of π_1 scales as a constant. The mixed correlations $\langle\phi\phi_1\rangle$ and $\langle\phi\phi_2\rangle$ scale as $1/\omega^{3/2}$, and the mixed correlations $\langle\phi\pi_1\rangle$ and $\langle\phi_{1,2}\pi_1\rangle$ scale as $1/\omega$ and $1/\omega^{1/2}$, respectively.

Defining the momentum- and frequency-dependent spin susceptibility by

$$\chi_s^{ij}(\boldsymbol{k},\boldsymbol{p};i\Omega_n) = \int d\boldsymbol{x}d\boldsymbol{y}e^{i\boldsymbol{k}\cdot\boldsymbol{x}-i\boldsymbol{p}\cdot\boldsymbol{y}}\int_0^{1/T} d\tau e^{-i\Omega_n\tau} \times\chi_s^{ij}(\boldsymbol{x},\boldsymbol{y};\tau), \tag{4.41}$$

we find that χ_s^{+-} and χ_s^{-+} reflect the strongest hydrodynamic contribution, which is given in terms of the $\phi-\phi$ correlation function at wave vector $\pm\boldsymbol{q}$,

$$\chi_s^{\pm\mp}(\boldsymbol{k},\boldsymbol{p};i\Omega_n) = \delta_{\boldsymbol{kp}}m_0^2\chi_{\phi\phi}(\boldsymbol{k}\pm\boldsymbol{q},i\Omega_n) + (\text{less leading terms}). \tag{4.42a}$$

The "less leading terms" in Eq. (4.42) reflect the terms proportional to c in Eq. (4.38a). They are either less singular than the leading term, which scales as $1/\omega^2$, or have a prefactor that is small by a factor of $cq \propto q^2$. χ_s^{++} and χ_s^{--} also are proportional to $\chi_{\phi\phi}$, but they are not diagonal in the momenta,

$$\chi_s^{\pm\pm}(\boldsymbol{k},\boldsymbol{p};i\Omega_n) = -\delta_{\boldsymbol{p},\boldsymbol{k}\pm2\boldsymbol{q}}m_0^2\chi_{\phi\phi}(\boldsymbol{k}\pm\boldsymbol{q},i\Omega_n). \tag{4.42b}$$

Only the terms with $\boldsymbol{k}=\boldsymbol{p}$ contribute to the neutron scattering cross section. Right and left circularly polarized neutrons will therefore see the hydrodynamic singularity only at wave vector $\boldsymbol{k}=\boldsymbol{q}$ and $\boldsymbol{k}=-\boldsymbol{q}$, respectively. Unpolarized neutrons will see symmetric contributions at $\boldsymbol{k}=\pm\boldsymbol{q}$. For instance, the xx component of the susceptibility tensor, $\chi_s^{11}=(\chi_s^{+-}+\chi_s^{-+}+\chi_s^{++}+\chi_s^{--})/4$ is given by

$$\chi_s^{11}(\boldsymbol{k},\boldsymbol{p};i\Omega_n) = \frac{m_0^2}{4}[\delta_{\boldsymbol{pk}}(\chi_{\phi\phi}(\boldsymbol{k}+\boldsymbol{q},i\Omega_n) + \chi_{\phi\phi}(\boldsymbol{k}-\boldsymbol{q},i\Omega_n)) - \delta_{\boldsymbol{p},\boldsymbol{k}+2\boldsymbol{q}}\chi_{\phi\phi}(\boldsymbol{k}+\boldsymbol{q},i\Omega_n) - \delta_{\boldsymbol{p},\boldsymbol{k}-2\boldsymbol{q}}\chi_{\phi\phi}(\boldsymbol{k}-\boldsymbol{q},i\Omega_n)]. \tag{4.43}$$

with the first term in the square brackets contributing to the neutron scattering cross section.

The longitudinal component χ_s^{33} is less singular than χ_s^{+-} since the contribution of ϕ to $(A^{-1}\delta M)_z$ is suppressed by a transverse gradient; see Eqs. (4.38b) and (4.39a). Accordingly, the leading hydrodynamic contribution to χ_s^{33} at $\boldsymbol{k}=\pm\boldsymbol{q}$ scales as $\langle\varphi_1\varphi_1\rangle \sim 1/\omega$. There is also a weak signature of the Goldstone mode in the vicinity of $\boldsymbol{k}=0$ due to the contribution of $\langle\pi_1\pi_1\rangle$ to χ_s^{33}, but this scales only as ω^0.

All of these results are in agreement with what one expects from Sec. II D.

V. DISCUSSION AND CONCLUSION

Let us summarize our results. We have developed a framework for a theoretical description of itinerant quantum helimagnets that is analogous to Hertz's treatment of ferromagnets.[26] We have analyzed this theory in the helically ordered phase at a mean-field and Gaussian level analogous to Stoner theory. As in the ferromagnetic case there is a split Fermi surface, with the splitting proportional to the amplitude of the helically modulated magnetization. We then focused on the Goldstone mode, or helimagnon, that results from the spontaneous breaking of the translational symmetry in the helical phase. We have found that the helimagnon is a propagating, weakly damped mode with a strongly anisotropic dispersion relation. The frequency scales linearly with the wave number for wave vectors parallel to the pitch of the helix, but quadratically for wave vectors in the transverse direction. In this sense the helimagnon behaves like an antiferromagnetic magnon in the longitudinal direction, but like a ferromagnetic one in the transverse direction. This anisotropy is analogous to the situation in chiral liquid crystals, and indeed the results of our microscopic theory are qualitatively reproduced by combining an educated guess of the statics, inferred from the liquid-crystal case, with a phenomenological time-dependent Ginzburg-Landau theory for the dynamics. The structure of the microscopic field theory is in one-to-one correspondence with the structure of the phenomenological theory. Particle-hole excitations provide a damping of the helimagnon, with a damping coefficient proportional to the pitch wave number to the fourth power.

Our continuum theory ignores the spin-orbit coupling of the electron spins to the underlying lattice which, in conjunction with crystal-field effects, will change the dispersion relation of the Goldstone mode at very small wave numbers or frequencies. In contrast to the case of ferromagnetic and antiferromagnetic magnons, however, breaking the spin rotational symmetry does not give the helimagnons a mass; it just changes the dispersion relation at unobservably small wave numbers, making it less soft. Consistent with this, soft helimagnons are observable by neutron scattering,[38] as are ferromagnetic and antiferromagnetic magnons. The neutron scattering cross section is proportional to the magnetic structure factor, which in turn is simply related to the spin susceptibility, which we have shown to be proportional to the helimagnon correlation function.

Let us now discuss some observable properties using parameter values appropriate for MnSi. MnSi has a Fermi temperature $T_F \approx 23\,200$ K,[39] a pitch wave number $q \approx 0.035$ Å^{-1},[40] and an effective electron mass, averaged over the Fermi surface, $m_e \approx 4m_0$,[41] with m_0 the free electron mass. In a nearly-free-electron model this leads to $k_F \approx 1.45$ Å^{-1} and $qv_F/k_B \approx 1000$ K. The value of the exchange splitting λ is less clear. The large ordered moment of about 0.4 μ_B per formula unit[11] suggests an exchange splitting that is a substantial fraction of T_F. This is hard to reconcile with the low Curie temperature $T_C = 29.5$ K at ambient pressure. Reference 41 found an exchange splitting $\lambda/k_B \approx 520$ K, which is hard to reconcile with the large ordered moment. We recall that the helical order is caused by the (weak) spin-orbit interaction, which suggests a clear separation of energy scales and, in particular, $\lambda \gg qv_F$. In judging such estimates one needs to keep in mind that MnSi is a fairly strong magnet (as evidenced by the large ordered moment) with a complicated Fermi surface with both electron and hole orbits, and a nearly-free-electron model as well as a weak-coupling Stoner picture is of limited applicability.

One question that arises is the value of qv_F/λ appropriate for MnSi (recall that our calculation is for $qv_F/\lambda \ll 1$). This hinges on the value of λ. If one accepts a sizable value of λ (in units of the Fermi temperature) as suggested by the large value of the ordered magnetic moment, then $qv_F/\lambda \ll 1$. If one accepts the much smaller value for λ obtained in Ref. 41, then $qv_F/\lambda \approx 1$. Even in the latter case we expect our considerations to still apply qualitatively, although the lack of a clear separation of energy scales would make a quantitative analysis more difficult.

The anisotropic helimagnon is well defined for wave numbers $|\boldsymbol{k}| < q$. In MnSi, $q \approx 0.035$ Å^{-1}, which is accessible by inelastic neutron scattering.[11] An estimate of the helimagnon excitation energy in MnSi at this wave number can be obtained from Ref. 42. In this experiment, a small magnetic field was used to destroy the helix. The resulting ferromagnetic magnons at a wave number equal to q had an energy of about 300 mK above the field-induced gap. An estimate of the helimagnon energy at the same wave number from Eq. (4.33b) yields the same order of magnitude if λ is a substantial fraction of the Fermi energy. The prediction is thus for an anisotropic helimagnon, which at a wave number on the order of q and an energy on the order of 300 mK, will cross over to a ferromagnetic magnon. The damping is expected to be weak, especially in systems with some quenched disorder, although in ultraclean systems it may be strongly wave vector dependent.[34]

One expects the low-energy helimagnon mode to have an appreciable effect on other observables such as the specific heat or the electrical resistivity. This is indeed the case, and we will discuss these effects in a separate paper.[12]

In conclusion, the present paper provides a general many-body formalism for itinerant quantum helimagnets, which can be used for calculating any observable of interest, with the single-particle Green function and the helimagnon propagator as building blocks. Observables of obvious interest include the specific heat, the quasiparticle relaxation time, and the resistivity. Calculations of these quantities within the framework of the present theory will be reported in a separate paper.[12]

ACKNOWLEDGMENTS

We thank the participants of the Workshop on Quantum Phase Transitions at the KITP at UCSB and, in particular, Christian Pfleiderer and Thomas Vojta for stimulating discussions. D.B. would like to thank Peter Böni, Christian Pfleiderer, and Willi Zwerger for their hospitality during a visit to the Technical University Munich. This work was supported by the NSF under Grant Nos. DMR-01-32555, DMR-01-32726, and PHY-99-07949 and by the DFG under Grant No. SFB 608.

APPENDIX A: ROTATIONAL-INVARIANCE-BREAKING TERMS IN THE GINZBURG-LANDAU EXPANSION

In addition to the term considered in Eq. (2.21), there are other terms that break the rotational symmetry and contribute to the same order in the spin-orbit interaction strength g_{SO}. The detailed structure of such terms in the action depends on the precise lattice structure. For definiteness we assume the cubic $P2_13$ space group realized, for instance, in MnSi.

The leading terms which break the rotational symmetry are of the form[6,7]

$$\delta S = \int d\boldsymbol{x}\boldsymbol{(}a_1\{[\partial_x^2 \boldsymbol{M}(\boldsymbol{x})]^2 + [\partial_y^2 \boldsymbol{M}(\boldsymbol{x})]^2 + [\partial_z^2 \boldsymbol{M}(\boldsymbol{x})]^2\} + g_{SO}^2\{a_2[\partial_x M_y(\boldsymbol{x})]^2 + a_3[\partial_x M_z(\boldsymbol{x})]^2 + \text{cycl}\} + g_{SO}^4 a_4\{[M_x(\boldsymbol{x})]^4 + [M_y(\boldsymbol{x})]^4 + [M_z(\boldsymbol{x})]^4\}\boldsymbol{)}. \tag{A1}$$

Here a_1, a_2, a_3, and a_4 are constants which remain finite for vanishing spin-orbit coupling, $g_{SO} \to 0$, and "cycl" denotes cyclic permutations of x, y, and z. Omitted terms like $(M_x^2 M_y^2 + \text{cycl})$ or $[(\partial_x M_x)^2 + \text{cycl}]$ can be obtained by adding rotationally invariant terms to δS. We note that the Dzyaloshinski-Moriya interaction—i.e. the constant c in Eq. (2.1), the pitch wave number q, and therefore all typical momenta—is *linear* in g_{SO}. Consequently, all terms in Eq. (A1) contribute only to order g_{SO}^4. They are therefore small compared to the energy gain obtained by forming the helical state, which is is of order $q^2 \propto g_{SO}^2$.

The main effect of δS is to pin the direction of the spiral to some high-symmetry direction: namely, either (1,1,1) and equivalent directions or (1,0,0) and equivalent directions.[6,7] In addition, they change the dispersion relation of the helical Goldstone mode at extremely small wave numbers. For one particular term this has been demonstrated in Sec. II E; all other terms have qualitatively the same effect. Notice that in a *ferromagnet* the effect on the Goldstone mode is stronger. For instance, the cubic anisotropy [the term with coupling constant a_4 in Eq. (A1)] gives the ferromagnetic magnons a true mass, leaving no soft modes. This is a result of the fact that in a ferromagnetic state the translational invariance is not spontaneously broken, while in a helimagnetic one it is.

APPENDIX B: THE REFERENCE ENSEMBLE SPIN SUSCEPTIBILITY

Substituting Eq. (4.13a) into Eq. (4.14b) and performing the spin traces yields

$$\begin{aligned}
\chi_0^{ij}(\boldsymbol{k},\boldsymbol{p};i\Omega_n) = \frac{-1}{V}\sum_{\boldsymbol{k}'} T\sum_{i\omega_m} \{&\delta_{\boldsymbol{k},\boldsymbol{p}}[(\Sigma_{aa}^{++})_{ij}a_+(\boldsymbol{k}'-\boldsymbol{k},\boldsymbol{q};i\omega_m - i\Omega_n)a_+(\boldsymbol{k}',\boldsymbol{q};i\omega_n) + (\Sigma_{aa}^{+-})_{ij}a_+(\boldsymbol{k}'-\boldsymbol{k},\boldsymbol{q};i\omega_m - i\Omega_n)a_-(\boldsymbol{k}',\boldsymbol{q};i\omega_n)\\
&+ (\Sigma_{aa}^{-+})_{ij}a_-(\boldsymbol{k}'-\boldsymbol{k},\boldsymbol{q};i\omega_m - i\Omega_n)a_+(\boldsymbol{k}',\boldsymbol{q};i\omega_n) + (\Sigma_{aa}^{--})_{ij}a_-(\boldsymbol{k}'-\boldsymbol{k},\boldsymbol{q};i\omega_m - i\Omega_n)a_-(\boldsymbol{k}',\boldsymbol{q};i\omega_n)\\
&+ (\Sigma_{bb}^{+-})_{ij}b_+(\boldsymbol{k}'-\boldsymbol{k},\boldsymbol{q};i\omega_m - i\Omega_n)b_-(\boldsymbol{k}'+\boldsymbol{q},\boldsymbol{q};i\omega_n) + (\Sigma_{bb}^{-+})_{ij}b_-(\boldsymbol{k}'-\boldsymbol{k},\boldsymbol{q};i\omega_m - i\Omega_n)b_+(\boldsymbol{k}'-\boldsymbol{q},\boldsymbol{q};i\omega_n)]\\
&+ \delta_{\boldsymbol{k}-\boldsymbol{q},\boldsymbol{p}}[(\Sigma_{ab}^{++})_{ij}a_+(\boldsymbol{k}'-\boldsymbol{k},\boldsymbol{q};i\omega_m - i\Omega_n)b_+(\boldsymbol{k}'-\boldsymbol{q},\boldsymbol{q};i\omega_n) + (\Sigma_{ab}^{-+})_{ij}a_-(\boldsymbol{k}'-\boldsymbol{k},\boldsymbol{q};i\omega_m - i\Omega_n)b_+(\boldsymbol{k}'-\boldsymbol{q},\boldsymbol{q};i\omega_n)\\
&+ (\Sigma_{ba}^{++})_{ij}b_+(\boldsymbol{k}'-\boldsymbol{k},\boldsymbol{q};i\omega_m - i\Omega_n)a_+(\boldsymbol{k}',\boldsymbol{q};i\omega_n) + (\Sigma_{ba}^{+-})_{ij}b_+(\boldsymbol{k}'-\boldsymbol{k},\boldsymbol{q};i\omega_m - i\Omega_n)a_-(\boldsymbol{k}',\boldsymbol{q};i\omega_n)]\\
&+ \delta_{\boldsymbol{k}+\boldsymbol{q},\boldsymbol{p}}[(\Sigma_{ab}^{+-})_{ij}a_+(\boldsymbol{k}'-\boldsymbol{k},\boldsymbol{q};i\omega_m - i\Omega_n)b_-(\boldsymbol{k}'+\boldsymbol{q},\boldsymbol{q};i\omega_n) + (\Sigma_{ab}^{--})_{ij}a_-(\boldsymbol{k}'-\boldsymbol{k},\boldsymbol{q};i\omega_m - i\Omega_n)b_-(\boldsymbol{k}'+\boldsymbol{q},\boldsymbol{q};i\omega_n)\\
&+ (\Sigma_{ba}^{-+})_{ij}b_-(\boldsymbol{k}'-\boldsymbol{k},\boldsymbol{q};i\omega_m - i\Omega_n)a_+(\boldsymbol{k}',\boldsymbol{q};i\omega_n) + (\Sigma_{ba}^{--})_{ij}b_-(\boldsymbol{k}'-\boldsymbol{k},\boldsymbol{q};i\omega_m - i\Omega_n)a_-(\boldsymbol{k}',\boldsymbol{q};i\omega_n)]\\
&+ \delta_{\boldsymbol{k}-2\boldsymbol{q},\boldsymbol{p}}(\Sigma_{bb}^{++})_{ij}b_+(\boldsymbol{k}'-\boldsymbol{k},\boldsymbol{q};i\omega_m - i\Omega_n)b_+(\boldsymbol{k}'-\boldsymbol{q},\boldsymbol{q};i\omega_n) + \delta_{\boldsymbol{k}+2\boldsymbol{q},\boldsymbol{p}}(\Sigma_{bb}^{--})_{ij}b_-(\boldsymbol{k}'-\boldsymbol{k},\boldsymbol{q};i\omega_m - i\Omega_n)b_-(\boldsymbol{k}'+\boldsymbol{q},\boldsymbol{q};i\omega_n)\}.
\end{aligned} \tag{B1}$$

The Σ symbols denote traces of Pauli matrices:

$$(\Sigma_{aa}^{++})_{ij} = \text{tr}(\sigma_i\sigma_+\sigma_-\sigma_j\sigma_+\sigma_-) = \begin{pmatrix} 0 & 0 & 0 \\ 0 & 0 & 0 \\ 0 & 0 & 1 \end{pmatrix}, \tag{B2a}$$

$$(\Sigma_{aa}^{+-})_{ij} = \text{tr}(\sigma_i\sigma_+\sigma_-\sigma_j\sigma_-\sigma_+) = \begin{pmatrix} 1 & -i & 0 \\ i & 1 & 0 \\ 0 & 0 & 0 \end{pmatrix}, \tag{B2b}$$

$$(\Sigma_{aa}^{-+})_{ij} = \text{tr}(\sigma_i\sigma_-\sigma_+\sigma_j\sigma_+\sigma_-) = \begin{pmatrix} 1 & i & 0 \\ -i & 1 & 0 \\ 0 & 0 & 0 \end{pmatrix}, \tag{B2c}$$

$$(\Sigma_{aa}^{--})_{ij} = \text{tr}(\sigma_i\sigma_-\sigma_+\sigma_j\sigma_-\sigma_+) = \begin{pmatrix} 0 & 0 & 0 \\ 0 & 0 & 0 \\ 0 & 0 & 1 \end{pmatrix}, \tag{B2d}$$

$$(\Sigma_{bb}^{+-})_{ij} = \text{tr}(\sigma_i\sigma_+\sigma_j\sigma_-) = \begin{pmatrix} 0 & 0 & 0 \\ 0 & 0 & 0 \\ 0 & 0 & -1 \end{pmatrix}, \tag{B2e}$$

$$(\Sigma_{bb}^{-+})_{ij} = \mathrm{tr}(\sigma_i\sigma_-\sigma_j\sigma_+) = \begin{pmatrix} 0 & 0 & 0 \\ 0 & 0 & 0 \\ 0 & 0 & -1 \end{pmatrix}, \tag{B2f}$$

$$(\Sigma_{ab}^{++})_{ij} = \mathrm{tr}(\sigma_i\sigma_+\sigma_-\sigma_j\sigma_+) = \begin{pmatrix} 0 & 0 & 1 \\ 0 & 0 & i \\ 0 & 0 & 0 \end{pmatrix}, \tag{B2g}$$

$$(\Sigma_{ab}^{-+})_{ij} = \mathrm{tr}(\sigma_i\sigma_-\sigma_+\sigma_j\sigma_+) = \begin{pmatrix} 0 & 0 & 0 \\ 0 & 0 & 0 \\ -1 & -i & 0 \end{pmatrix}, \tag{B2h}$$

$$(\Sigma_{ba}^{++})_{ij} = \mathrm{tr}(\sigma_i\sigma_+\sigma_j\sigma_+\sigma_-) = \begin{pmatrix} 0 & 0 & 0 \\ 0 & 0 & 0 \\ 1 & i & 0 \end{pmatrix}, \tag{B2i}$$

$$(\Sigma_{ba}^{+-})_{ij} = \mathrm{tr}(\sigma_i\sigma_+\sigma_j\sigma_-\sigma_+) = \begin{pmatrix} 0 & 0 & -1 \\ 0 & 0 & -i \\ 0 & 0 & 0 \end{pmatrix}, \tag{B2j}$$

$$(\Sigma_{ab}^{+-})_{ij} = \mathrm{tr}(\sigma_i\sigma_+\sigma_-\sigma_j\sigma_-) = \begin{pmatrix} 0 & 0 & 0 \\ 0 & 0 & 0 \\ 1 & -i & 0 \end{pmatrix}, \tag{B2k}$$

$$(\Sigma_{ab}^{--})_{ij} = \mathrm{tr}(\sigma_i\sigma_-\sigma_+\sigma_j\sigma_-) = \begin{pmatrix} 0 & 0 & -1 \\ 0 & 0 & i \\ 0 & 0 & 0 \end{pmatrix}, \tag{B2l}$$

$$(\Sigma_{ba}^{-+})_{ij} = \mathrm{tr}(\sigma_i\sigma_-\sigma_j\sigma_+\sigma_-) = \begin{pmatrix} 0 & 0 & 1 \\ 0 & 0 & -i \\ 0 & 0 & 0 \end{pmatrix}, \tag{B2m}$$

$$(\Sigma_{ba}^{--})_{ij} = \mathrm{tr}(\sigma_i\sigma_-\sigma_j\sigma_-\sigma_+) = \begin{pmatrix} 0 & 0 & 0 \\ 0 & 0 & 0 \\ -1 & i & 0 \end{pmatrix}, \tag{B2n}$$

$$(\Sigma_{bb}^{++})_{ij} = \mathrm{tr}(\sigma_i\sigma_+\sigma_j\sigma_+) = \begin{pmatrix} 1 & i & 0 \\ i & -1 & 0 \\ 0 & 0 & 0 \end{pmatrix}, \tag{B2o}$$

$$(\Sigma_{bb}^{--})_{ij} = \mathrm{tr}(\sigma_i\sigma_-\sigma_j\sigma_-) = \begin{pmatrix} 1 & -i & 0 \\ -i & -1 & 0 \\ 0 & 0 & 0 \end{pmatrix}. \tag{B2p}$$

APPENDIX C: THE FUNCTIONS $f_{\phi\phi}$, f_{11}, f_{12}, g_{11}, AND $h_{\phi 1}$

In this appendix we show how to evaluate the functions $f_{\phi\phi}$, f_{11}, f_{12}, and $h_{\phi 1}$ defined in Eqs. (4.18c), (4.18d), (4.18e), (4.18f), (4.18g), and (4.30) in the limit of long wavelengths and small frequencies.

1. Function $f_{\phi\phi}$

We start with the expression for $\varphi_{\phi\phi}$ in terms of Green functions given in Eq. (4.18f). By symmetrizing the dependence on $\boldsymbol{k}$ and $\boldsymbol{q}$, performing the sum over Matsubara frequencies and doing a partial fraction decomposition, $\varphi_{\phi\phi}$ can be written

$$\varphi_{\phi\phi}(\boldsymbol{k},i\Omega_n) = \varphi_{\phi\phi}^{(+)}(\boldsymbol{k},i\Omega_n) + \varphi_{\phi\phi}^{(+)}(-\boldsymbol{k},-i\Omega_n) + \varphi_{\phi\phi}^{(-)}(\boldsymbol{k},i\Omega_n) - \varphi_{\phi\phi}^{(-)}(-\boldsymbol{k},-i\Omega_n). \tag{C1a}$$

From Eq. (4.18c) we have

$$f_{\phi\phi}(\boldsymbol{k},i\Omega_n) = 2[\varphi_{\phi\phi}^{(+)}(\boldsymbol{k},i\Omega_n) + \varphi_{\phi\phi}^{(+)}(-\boldsymbol{k},-i\Omega_n)]. \tag{C1b}$$

That is, $f_{\phi\phi}$ is given by the symmetric part of $\varphi_{\phi\phi}$ alone. The antisymmetric part $\varphi_{\phi\phi}^{(-)}$ does not contribute, but we list it here for completeness:

$$\varphi_{\phi\phi}^{(-)}(\boldsymbol{k},i\Omega_n) = \frac{-1}{4V}\sum_{\boldsymbol{p}}\Bigg\{\frac{(\boldsymbol{q}\cdot\boldsymbol{p}_-)w_+ - (\boldsymbol{q}\cdot\boldsymbol{p}_+)w_-}{2m_e w_+ w_-}\left[\frac{f(\xi_-^q - w_-)}{i\Omega_n - \boldsymbol{k}\cdot\boldsymbol{p}/m_e + w_+ - w_-} - \frac{f(\xi_-^q + w_-)}{i\Omega_n - \boldsymbol{k}\cdot\boldsymbol{p}/m_e - w_+ + w_-}\right] + \frac{(\boldsymbol{q}\cdot\boldsymbol{p}_-)w_+ + (\boldsymbol{q}\cdot\boldsymbol{p}_+)w_-}{2m_e w_+ w_-}\left[\frac{f(\xi_-^q - w_-)}{i\Omega_n - \boldsymbol{k}\cdot\boldsymbol{p}/m_e - w_+ - w_-} - \frac{f(\xi_-^q + w_-)}{i\Omega_n - \boldsymbol{k}\cdot\boldsymbol{p}/m_e + w_+ + w_-}\right]\Bigg\}. \tag{C1c}$$

The symmetric part $\varphi^{(+)}$ consists of two parts that are structurally distinct,

$$\varphi_{\phi\phi}^{(+)}(\boldsymbol{k},i\Omega_n) = \varphi_{\phi\phi}^{(1)}(\boldsymbol{k},i\Omega_n) + \varphi_{\phi\phi}^{(2)}(\boldsymbol{k},i\Omega_n), \tag{C1d}$$

where

$$\varphi_{\phi\phi}^{(1)}(\boldsymbol{k},i\Omega_n) = \frac{-1}{4V}\sum_{\boldsymbol{p}}\frac{w_+w_- + \lambda^2 + g(\boldsymbol{p})}{w_+w_-}\left[\frac{f(\xi_-^q - w_-)}{i\Omega_n - \boldsymbol{k}\cdot\boldsymbol{p}/m_e - w_+ - w_-} + \frac{f(\xi_-^q + w_-)}{i\Omega_n - \boldsymbol{k}\cdot\boldsymbol{p}/m_e + w_+ + w_-}\right], \tag{C1e}$$

$$\varphi_{\phi\phi}^{(2)}(\boldsymbol{k},i\Omega_n) = \frac{-1}{4V}\sum_{\boldsymbol{p}}\frac{w_+w_- - \lambda^2 - g(\boldsymbol{p})}{w_+w_-}\left[\frac{f(\xi_-^q - w_-)}{i\Omega_n - \boldsymbol{k}\cdot\boldsymbol{p}/m_e + w_+ - w_-} + \frac{f(\xi_-^q + w_-)}{i\Omega_n - \boldsymbol{k}\cdot\boldsymbol{p}/m_e - w_+ + w_-}\right]. \tag{C1f}$$

In these expressions $\xi^q_\pm = \xi_{p_\pm} + q^2/8m_e$, $\boldsymbol{p}_\pm = \boldsymbol{p} \pm \boldsymbol{k}/2$, and $w_\pm = w(\boldsymbol{p}_\pm)$ with

$$w(\boldsymbol{p}) = \sqrt{\frac{(\boldsymbol{q}\cdot\boldsymbol{p})^2}{4m_e^2} + \lambda^2} \tag{C1g}$$

and

$$g(\boldsymbol{p}) = \frac{1}{4m_e^2}\left((\boldsymbol{q}\cdot\boldsymbol{p})^2 - \frac{1}{4}(\boldsymbol{q}\cdot\boldsymbol{k})^2\right). \tag{C1h}$$

$\varphi^{(1)}_{\phi\phi}$ and $\varphi^{(2)}_{\phi\phi}$ are both generalized Lindhard functions. For $\lambda=0$ they combine to form a Lindhard function at wave vector $\boldsymbol{k}+\boldsymbol{q}$, while, for $\boldsymbol{q}=0$, $\varphi^{(2)}_{\phi\phi}$ vanishes and $\varphi^{(1)}_{\phi\phi}$ turns into the function that determines the ferromagnetic magnon.[32] A structural difference between them is that in $\varphi^{(1)}_{\phi\phi}$ the hydrodynamic singularity at $\boldsymbol{k}=i\Omega_n=0$ that is characteristic for the Lindhard function is protected by λ, while in $\varphi^{(2)}_{\phi\phi}$ this is not the case.

The remaining wave vector integral is difficult, and we evaluate it only in the limit $\lambda \gg qv_F$. The Fermi functions in Eqs. (C1e) and (C1f) pin the integration momentum $\boldsymbol{p}$ to a shifted Fermi surface. For $\lambda > qv_F$ one can therefore perform a straightforward expansion of the integrand in powers of qv_F/λ. For $\varphi^{(1)}$ the leading term is the $\boldsymbol{q}=0$ contribution. Specifically, in this limit,

$$[w_+w_- + \lambda^2 + g(\boldsymbol{p})]/w_+w_- \to 2, \tag{C2}$$

and the calculation reduces to the ferromagnetic case. For $k \ll k_F$ and $|\Omega_n| \ll \lambda$, the result is

$$\varphi^{(1)}_{\phi\phi}(\boldsymbol{k},i\Omega_n) = \varphi^{(1)}_{\phi\phi}(0,i0) + N_F\left[-\frac{1}{3}\left(\frac{\boldsymbol{k}}{2k_F}\right)^2 + \left(\frac{i\Omega_n}{2\lambda}\right)^2\right]. \tag{C3}$$

For $\varphi^{(2)}$ the leading term is of $O(q^2)$, since

$$[w_+w_- - \lambda^2 - g(\boldsymbol{p})]/w_+w_- \to (\boldsymbol{q}\cdot\boldsymbol{k})^2/8m_e^2\lambda^2, \tag{C4}$$

and the integral is reduces to a Lindhard function. The nonhydrodynamic part provides only corrections of $O((qv_F/\lambda)^2)$ to $\varphi^{(1)}$, but the hydrodynamic part is qualitatively new and must be kept. We find

$$\varphi^{(2)}(\boldsymbol{k},i\Omega_n) = \varphi^{(2)}(\boldsymbol{k},i0) - N_F\frac{\pi}{32}\frac{(\boldsymbol{q}\cdot\boldsymbol{k})^2}{m_e^2\lambda^2}\frac{|\Omega_n|}{v_F|\boldsymbol{k}|}, \tag{C5}$$

which is valid for $|\Omega_n| \ll v_F k$. Combining these results yields Eq. (4.20a) with coefficients appropriate for the case $\lambda \gg qv_F$. Corrections are of $O((qv_F/\lambda)^2)$.

2. Functions f_{11}, f_{12}, and g_{11}

In order to calculate φ_{11}, Eq. (4.18g), it is convenient to consider $\varphi_{11}(\boldsymbol{k}-\boldsymbol{q},i\Omega_n)$, which can be written in a form similar to $\varphi_{\phi\phi}(\boldsymbol{k},i\Omega_n)$: namely,

$$\varphi_{11}(\boldsymbol{k}-\boldsymbol{q},i\Omega_n) = \varphi^{(1)}_{11}(\boldsymbol{k}-\boldsymbol{q},i\Omega_n) + \varphi^{(2)}_{11}(\boldsymbol{k}-\boldsymbol{q},i\Omega_n), \tag{C6a}$$

where

$$\varphi^{(1)}_{11}(\boldsymbol{k}-\boldsymbol{q},i\Omega_n) = \frac{-1}{8V}\sum_{\boldsymbol{p}}\frac{w_+w_- - g(\boldsymbol{p}) + \lambda^2}{w_+w_-}\left[\frac{f(\xi^q_- - w_-) - f(\xi^q_+ + w_+)}{i\Omega_n - \boldsymbol{k}\cdot\boldsymbol{p}/m_e - w_+ - w_-} + \frac{f(\xi^q_- + w_-) - f(\xi^q_+ - w_+)}{i\Omega_n - \boldsymbol{k}\cdot\boldsymbol{p}/m_e + w_+ + w_-}\right], \tag{C6b}$$

$$\varphi^{(2)}_{11}(\boldsymbol{k}-\boldsymbol{q},i\Omega_n) = \frac{-1}{8V}\sum_{\boldsymbol{p}}\frac{w_+w_- + g(\boldsymbol{p}) - \lambda^2}{w_+w_-}\left[\frac{f(\xi^q_- - w_-) - f(\xi^q_+ - w_+)}{i\Omega_n - \boldsymbol{k}\cdot\boldsymbol{p}/m_e + w_+ - w_-} + \frac{f(\xi^q_- + w_-) - f(\xi^q_+ + w_+)}{i\Omega_n - \boldsymbol{k}\cdot\boldsymbol{p}/m_e - w_+ + w_-}\right]. \tag{C6c}$$

To evaluate these integrals we again assume $\lambda \gg qv_F$. In this limit,

$$[w_+w_- - g(\boldsymbol{p}) + \lambda^2]/w_+w_- \to 2, \tag{C7}$$

and the integral again reduces to the ferromagnetic case. The result is

$$\varphi^{(1)}_{11}(\boldsymbol{k}-\boldsymbol{q},i\Omega_n) = \varphi_{11}(\boldsymbol{q},i0) + \frac{N_F}{2}\left[-\frac{1}{3}\left(\frac{\boldsymbol{k}}{2k_F}\right)^2 + \left(\frac{i\Omega_n}{2\lambda}\right)^2\right]. \tag{C8a}$$

Shifting $\boldsymbol{k}$ by $\boldsymbol{q}$, we find

$$\varphi^{(1)}_{11}(\boldsymbol{k},i\Omega_n) = \varphi^{(1)}_{11}(0,i0) + \frac{N_F}{2}\left[-\frac{2}{3}\frac{\boldsymbol{k}\cdot\boldsymbol{q}}{(2k_F)^2} - \frac{1}{3}\left(\frac{k}{2k_F}\right)^2 + \left(\frac{i\Omega_n}{2\lambda}\right)^2\right]. \tag{C8b}$$

For $\varphi^{(2)}_{11}$ we need

$$[w_+w_- + g(\boldsymbol{p}) - \lambda^2]/w_+w_- \to (\boldsymbol{q}\cdot\boldsymbol{p})^2/2m_e^2\lambda^2. \tag{C9}$$

In contrast to Eq. (C4), this is quadratic in the integration variable $\boldsymbol{p}$. $\varphi^{(2)}_{11}$ therefore is a stress correlation function. It has a hydrodynamic contribution of the same functional form as the Lindhard function, but only the transverse (with respect to $\boldsymbol{k}$) components contribute to it. The nonhydrodynamic contributions are again subleading compared to $\varphi_{11}^{(1)}$. One finds

$$\varphi_{11}^{(2)}(\boldsymbol{k}-\boldsymbol{q},i\Omega_n)=\varphi_{11}^{(2)}(\boldsymbol{k}-\boldsymbol{q},i0)+N_{\mathrm{F}}\frac{\pi}{32}\frac{v_{\mathrm{F}}q}{\lambda}\frac{q\boldsymbol{k}_\perp^2}{|\boldsymbol{k}|^3}\frac{|\Omega_n|}{\lambda}, \tag{C10a}$$

and after shifting the momentum we obtain

$$\varphi_{11}^{(2)}(\boldsymbol{k},i\Omega_n)=\varphi_{11}^{(2)}(\boldsymbol{k},i0)+N_{\mathrm{F}}\frac{\pi}{32}\frac{v_{\mathrm{F}}q}{\lambda}\frac{\boldsymbol{k}_\perp^2}{q^2}\frac{|\Omega_n|}{\lambda}. \tag{C10b}$$

Using these results in Eqs. (4.18d), (4.18e), and (4.29c) we obtain Eqs. (4.20b), (4.20c), and (4.30a), respectively.

3. Functions $h_{\phi 1}$

Finally, the function $\eta_{\phi 1}$, which is defined by Eq. (4.29e) and determines $h_{\phi 1}$ according to Eq. (4.29d), can be written

$$\eta_{\phi 1}(\boldsymbol{k},i\Omega_n)=\eta_{\phi 1}^{(1)}(\boldsymbol{k},i\Omega_n)+\eta_{\phi 1}^{(2)}(\boldsymbol{k},i\Omega_n), \tag{C11a}$$

where

$$\eta_{\phi 1}^{(1)}(\boldsymbol{k},i\Omega_n)=\frac{-\lambda}{V}\sum_{\boldsymbol{p}}\frac{w_+ + w_-}{w_+ w_-}\left[\frac{f(\xi_-^q - w_-)-f(\xi_+^q + w_+)}{i\Omega_n-\boldsymbol{p}\cdot\boldsymbol{k}/m_{\mathrm{e}}-w_+-w_-} - \frac{f(\xi_-^q + w_-)-f(\xi_+^q - w_+)}{i\Omega_n-\boldsymbol{p}\cdot\boldsymbol{k}/m_{\mathrm{e}}+w_++w_-}\right], \tag{C11b}$$

$$\eta_{\phi 1}^{(2)}(\boldsymbol{k},i\Omega_n)=\frac{-\lambda}{V}\sum_{\boldsymbol{p}}\frac{w_+ - w_-}{w_+ w_-}\left[\frac{f(\xi_-^q - w_-)-f(\xi_+^q - w_+)}{i\Omega_n-\boldsymbol{p}\cdot\boldsymbol{k}/m_{\mathrm{e}}+w_+-w_-} - \frac{f(\xi_-^q + w_-)-f(\xi_+^q + w_+)}{i\Omega_n-\boldsymbol{p}\cdot\boldsymbol{k}/m_{\mathrm{e}}+w_+-w_-}\right]. \tag{C11c}$$

Using the same techniques as above we find, in the limit $\lambda \gg qv_{\mathrm{F}}$,

$$\eta_{\phi 1}^{(1)}(\boldsymbol{k},i\Omega_n)=4N_{\mathrm{F}}\frac{i\Omega_n}{\lambda}. \tag{C11d}$$

$\eta_{\phi 1}^{(2)}$ is proportional to $N_{\mathrm{F}}(i\Omega_n/\lambda)(\boldsymbol{q}\cdot\boldsymbol{k})^2/k_{\mathrm{F}}^2\boldsymbol{k}^2$ and hence is small compared to $\eta_{\phi 1}^{(1)}$ by a factor of q^2/k_{F}^2. These results yield Eq. (4.30b).

---

[1] C. Kittel, *Introduction to Solid State Physics* (Wiley, New York, 1996), Chap. 15.

[2] D. Forster, *Hydrodynamic Fluctuations, Broken Symmetry, and Correlation Functions* (Benjamin, Reading, MA, 1975).

[3] J. Zinn-Justin, *Quantum Field Theory and Critical Phenomena* (Oxford University Press, Oxford, 1996).

[4] I. E. Dzyaloshinski, J. Phys. Chem. Solids **4**, 241 (1958).

[5] T. Moriya, Phys. Rev. **120**, 91 (1960).

[6] P. Bak and M. H. Jensen, J. Phys. C **13**, L881 (1980).

[7] O. Nakanishi, A. Yanase, A. Hasegawa, and M. Kataoka, Solid State Commun. **35**, 995 (1980).

[8] Y. Ishikawa, K. Tajima, D. Bloch, and M. Roth, Solid State Commun. **19**, 525 (1976).

[9] C. Pfleiderer, G. J. McMullan, S. R. Julian, and G. G. Lonzarich, Phys. Rev. B **55**, 8330 (1997).

[10] C. Pfleiderer, S. R. Julian, and G. G. Lonzarich, Nature (London) **414**, 427 (2001).

[11] C. Pfleiderer, D. Reznik, L. Pintschovius, H. v. Löhneysen, M. Garst, and A. Rosch, Nature (London) **427**, 227 (2004).

[12] D. Belitz, T. R. Kirkpatrick, and A. Rosch (unpublished).

[13] T. R. Kirkpatrick and D. Belitz, Phys. Rev. B **72**, 180402(R) (2005).

[14] P. Chaikin and T. C. Lubensky, *Principles of Condensed Matter Physics* (Cambridge University, Cambridge, MA, 1995), Chap. 6.2.

[15] P. G. de Gennes and J. Prost, *The Physics of Liquid Crystals* (Clarendon, Oxford, 1993).

[16] This expectation pertains in particular to the static properties. The dynamics in general and the damping of the mode in particular can be different and will be affected by the presence of fermionic quasiparticles in metallic helimagnets.

[17] P. Chaikin and T. C. Lubensky, Ref. 14, Chap. 6.3.

[18] Strictly speaking, this result implies that there is no true long-range helical order at nonzero temperatures, for the same reason for which there is no true long-range order in smectic liquid crystals (Ref. 17) or in a classical *xy* magnet in two dimensions (Ref. 43). We will ignore this effect, which becomes relevant only at extremely long wavelengths.

[19] T. C. Lubensky, Phys. Rev. A **6**, 452 (1972).

[20] S.-K. Ma, *Modern Theory of Critical Phenomena* (Benjamin, Reading, MA, 1976), Chap. XIII.

[21] For simplicity we ignore the difference between the phase ϕ and the generalized phase u. This is of no consequence since the correct rotational invariance is implicit in the effective action $S_{\mathrm{eff}}[u]$, which ultimately determines the dynamics of u.

[22] In principle one can imagine r_0 to become negative as a function of the coupling strength, which could lead to coexisting ferromagnetic and helical order. We will see later that this does not happen in the specific model we will consider, and we ignore this possibility.

[23] Note that restoring the rotational invariance by putting $b=0$ does not lead to additional Goldstone modes. The reason is that small fluctuations $\delta\boldsymbol{q}$ of the pitch vector lead to large changes of the order parameter, $\delta\boldsymbol{M}\propto\boldsymbol{x}\,\delta\boldsymbol{q}$ for large $\boldsymbol{x}$. This is the same effect that ensures the absence of a $\boldsymbol{k}_\perp^2$ term in the dispersion relation, and it is reminiscient of the Anderson-Higgs mechanism.

[24] J. Schmalian and M. Turlakov, Phys. Rev. Lett. **93**, 036405 (2004).

[25] This restriction is necessary to avoid an illegal increase in the number of degrees of freedom when the real field φ is represented in terms of two real fields φ_1 and φ_2.

[26] J. Hertz, Phys. Rev. B **14**, 1165 (1976).

[27] I. Fischer and A. Rosch, Europhys. Lett. **68**, 93 (2004).

[28] S.-K. Ma, Ref. 20, Chap. IX.7.

[29] J. Zinn-Justin, Ref. 3, Chap. 13.4.
[30] Here we keep only terms that couple flucuations at the same wave vector and neglect couplings between wave vectors that differ by multiples of $\boldsymbol{q}$. This is sufficient to determine the static properties of the helimagnon, but it precludes taking the ferromagnetic limit $\boldsymbol{q} \to 0$. See also Sec. IV D and Ref. 33.
[31] J. Zinn-Justin, Ref. 3, Chap. 30.
[32] D. Belitz, T. R. Kirkpatrick, A. J. Millis, and T. Vojta, Phys. Rev. B **58**, 14155 (1998).
[33] This additive procedure is valid as long as $\boldsymbol{q} \neq 0$ and for wave numbers smaller than $|\boldsymbol{q}|$. As Sec. IV C 3 shows, the phase fluctuations correctly turn into the ferromagnetic soft modes as $\boldsymbol{q} \to 0$, so no $\boldsymbol{k}=0$ modes must be added in the ferromagnetic limit. See also Ref. 30.
[34] In a clean system, this result hinges on the spherical Fermi surface we have assumed. A generic band structure leads to an overdamping of the mode in certain directions in momentum space [A. Rosch (unpublished)]. On the other hand, even small amounts of quenched disorder qualitatively *weaken* the damping; see Sec. IV E 2.
[35] A. A. Abrikosov, L. P. Gorkov, and I. E. Dzyaloshinski, *Methods of Quantum Field Theory in Statistical Physics* (Dover, New York, 1963), Sec. 39.2.
[36] G. Shirane, R. Cowley, C. Majkrzak, J. B. Sokoloff, B. Pahonis, C. H. Perry, and Y. Ishikawa, Phys. Rev. B **28**, 6251 (1983).
[37] M. Ishida, Y. Endoh, S. Mitsuda, Y. Ishikawa, and M. Tanaka, J. Phys. Soc. Jpn. **54**, 2975 (1985).
[38] B. Roessli, P. Böni, W. Fischer, and Y. Endoh, Physica B **345**, 124 (2004).
[39] O. Nakanishi, A. Yanase, and A. Hasegawa, J. Magn. Magn. Mater. **15–18**, 879 (1980).
[40] Y. Ishikawa, Y. Noda, Y. J. Uemura, C. F. Majkrzak, and G. Shirane, Phys. Rev. B **31**, 5884 (1985).
[41] L. Taillefer, G. Lonzarich, and P. Strange, J. Magn. Magn. Mater. **54–57**, 957 (1986).
[42] F. Semadeni, P. Böni, Y. Endoh, B. Roessli, and G. Shirane, Physica B **267**, 248 (1999).
[43] N. D. Mermin and H. Wagner, Phys. Rev. Lett. **17**, 1133 (1966).